Development and characterization of ketorolac tromethamine osmotic pump tablets

A.A. Ali*, O.M. Sayed

Department of Pharmaceutics and Industrial Pharmacy, Faculty of Pharmacy, Beni Suef University, Egypt
*Correspondence: dr_adelahmedali@yahoo.com

The aim of the present study was to prepare and evaluate elementary osmotic pump tablets (OPT) of ketorolac tromethamine (KT). Because of its high potency, short half-life and excellent water solubility it would appear to be the drug of choice for these formulations. Twenty OPT formulae were prepared and subjected to release-rate study and the release data were analyzed to determine the drug release order. Compatibility study between KT and the used excipients was carried out also scanning electron microscopy in order to elucidate the microporous nature of the tablet surfaces. The effects of an increase in weight, agitation intensity, pH and type of coating polymer on drug release from the optimal formulation (OPT-19) were studied. It was found that the optimal OPT formula was able to deliver KT at a zero-order for up to 12 h independent of both release media and agitation rates; the effect of type of coating polymer was not significant.

Key words: Ketorolac tromethamine – Cellulose acetate – Osmotic pump tablets – Semi-permeable membrane – Zero-order release.

Controlled drug delivery is an important factor in pharmaceutical development, due to increased patient compliance and tolerability with prescribed dosing regimens [1-2]. Oral controlled drug delivery systems can provide continuous delivery of drugs at predictable and reproducible rates throughout GI transit [3-5]. Also, due to a simplified dosing schedule, reduced side effects and greater patient convenience it provides greater effectiveness in the treatment of chronic conditions [6].

Osmotic systems that utilize the principle of osmotic pressure for controlled delivery of drug are the most promising systems used for controlled drug delivery [7-9]. Osmotic pump systems offer many advantages; for instance, they (i) are easily formulated and simple in operation, (ii) improve patient compliance by reducing dosing frequency, (iii) provide good *in vitro*/*in vivo* correlation, (iv) and their industrial adaptability and production scale-up is easy [10] .

Various types of osmotic pumps and formulation aspects have been reviewed and defined such as elementary osmotic pump systems, push-pull osmotic pump systems, controlled porosity osmotic pump systems, floating elementary osmotic pumps systems, and osmotic bursting osmotic pump systems [11-16].

Of the different types of oral osmotic systems reported in the literature, elementary osmotic pump (EOP) systems are the most commercially important osmotic devices, and more than 240 patents have been devoted due to simple structure and high efficiency [17-18].

Elementary osmotic pump systems are basically consisted of an osmotically active core surrounded by a semipermeable membrane and a small orifice drilled through the coating [19]. When these systems are exposed to an aqueous environment, the difference in osmotic pressure between the inside of the device and environment draws water through the semipermeable membrane. The saturated drug solution flows through the small orifice as a result of increased inner hydrostatic pressure. The process of drug release continues at a constant rate until the entire solid drug has been dissolved [19].

Both poorly soluble and water soluble drugs can be delivered at a controlled rate using osmotically controlled drug delivery systems [20]. Normally, the osmotic pump systems deliver 60-80 % of its content at a constant rate and there is a short lag time of 30-60 min as the system hydrates before zero order drug release from the systems is obtained [21]. Drug release from these systems is independent of pH and hydrodynamic conditions of the GI tract to a large extent, and release characteristics can be easily adjusted by optimizing the parameters of the delivery system [22].

Procardia XL and Adalat CR (nifedipine), Acutrium (phenylpropanolamine), Minipress XL (prazocine) and Volmax (salbutamol) are examples of elementary osmotic pump systems available on the market [22, 23].

Ketorolac tromethamine is a potent non-steroidal anti-inflammatory drug acting by inhibiting the synthesis of prostaglandins and is used in the management of moderate to severe pain [24]. Oral bioavailability of the drug is reported to be 90 %, with a very low first pass metabolism. Due to its short biological half life (4-6 h), frequent dosing is required to alleviate pain in postoperative patients [25].

No attempts have yet been made to formulate ketorolac tromethamine into osmotic pump tablets, the aim of the present study, Because of its high potency, excellent water solubility and lack of irritation to mucosal tissue [26], KT would appear to be of choice for formulation in elementary osmotic pump systems. Hence, the present work was aimed at preparing and evaluating an oral osmotic delivery system of KT and characterizing *in vitro* parameters, and directed towards achieving a better therapeutic effect and bioavailability of this drug.

I. MATERIALS

Ketorolac tromethamine was kindly supplied by El-Amerya pharmaceutical company (Egypt), Cellulose acetate (39.8 wt. % acetyl content. average MN ~ 30,000), cellulose acetate propionate (average MN ~ 25,000) and cellulose acetate butyrate (average MN ~ 65,000) were purchased from Sigma-Aldrich Company (United States), Compressol SM and sodium stearyl fumarate (Lubripharm SSF) were obtained as gift samples from SPI Pharma (United States), dibutyl phthalate and polyethylene glycol (PEG-400) were purchased from Fluka (Germany). All other chemicals and solvents were of analytical grades.

II. METHODOLOGY

1. Compatibility of KT with the used excipients

1.1. Differential scanning calorimetry

Samples of 5 mg of pure KT and its binary mixtures with the used excipients were placed into pierced aluminum containers and analyzed

by a DS Calorimeter (Setaram Labsys TG-DSC16). The studies were performed in the temperature range of 25 to 250 °C with a heating rate of 10 °C/min under nitrogen gas atmosphere. The peak temperatures were determined after calibration with purified indium 99.9 %.

1.2. Fourier-transform infrared spectroscopy

The IR spectra of pure KT and the binary mixtures were recorded on an IR spectro-photometer (Shimadzu IR-435, Kyoto, Japan). Samples weighing about 2-3 mg were mixed with about 400 mg of dry KBr and compressed into discs. The IR spectra were recorded at a scanning range of 400-4000 cm^{-1} and a resolution of 4 cm^{-1}.

2. Preparation of KT osmotic pump tablets

2.1. Preparation of KT core tablets

Four formulae (CO-1 to CO-4) containing 30 mg KT were prepared according to *Table I* as follow: firstly all ingredients were passed through sieve No. 60, and the calculated amounts of the drug, sodium chloride (as osmotic agent) and Compressol (as a filler) were mixed well then converted into wet mass using 5 % w/v PVP solution in isopropyl alcohol. The mass was forced through sieve No. 18 and the obtained granules were dried at 40 °C for 1 h. The dried granules were ground and the fraction that passed through sieve No. 40 and retained on sieve No. 60 was used; 1 % Lubripharm (as a lubricant) was added and mixed well.

By means of a single punch machine fitted with a concave 10 mm punch and die set, tablets of 300 mg were obtained. The target tablet hardness was adjusted to be in the range of 50 to 60 Newton using a tablet hardness tester (DR-Schlenger, Pharmaton, United States).

2.2. Characterization of the prepared core tablets

Ten tablets from each formula were individually weighed accurately and their average weight was calculated and presented as mean ± SD (*Table II*).

The diameter and thickness of ten randomly selected tablets from each formula were measured using an electronic digital vernier caliper (Shanghai, China). Results were reported as the mean ± SD (*Table II*).

Table I - Composition of different ketorolac tromethamine core tablets.

Ingredients (mg)	Core code			
	CO-1	CO-2	CO-3	CO-4
Ketorolac tromethamine	30	30	30	30
Sodium chloride	0	60	120	180
Sodium stearyl fumarate	3	3	3	3
Compressol SM up to	300 mg	300 mg	300 mg	300 mg

Table II - Data of average weight, thickness, diameter and friability of different ketorolac tromethamine core tablets.

For-mula code	Average weight (mg ± SD)	Thickness (mm ± SD)	Diameter (mm ± SD)	Friability (% fine)
CO-1	301 ± 0.025	3.69 ± 0.026	10.10 ± 0.018	0.147
CO-2	300 ± 0.085	3.49 ± 0.047	10.09 ± 0.014	0.160
CO-3	301 ± 0.048	3.25 ± 0.057	10.11 ± 0.019	0.245
CO-4	298 ± 0.089	3.13 ± 0.032	10.08 ± 0.004	0.213

Table III - Composition of different coating solutions used in preparation of ketorolac tromethamine OPTs (% w/v).

Ingredients	Coat code				
	CT-1	CT-2	CT-3	CT-4	CT-5
Cellulose acetate	5	5	5	5	5
Dibutyl phthalate	1	2	2	2	2
PEG-400	0	0	0.5	1.5	2.5

Friability of the tablets from each formula was calculated as follows: ten tablets were accurately weighed (W_1) and placed in the drum of the friabilator (Pharma Test, Germany) and rotated at 25 rpm for a period of 4 min and then reweighed (W_2). The percent loss in weight was calculated from the following equation and taken as a measure of friability [27]:

$$\% \text{ weight loss} = [(W_1 - W_2)/W_1] \times 100$$

2.3. Coating of KT core tablets

According to *Table III*, five coating solutions assigned CT-1 to CT-5 were prepared. A film former (cellulose acetate, 5 % w/v) and a plasticizer (dibutyl phthalate, 1 or 2 % w/v) and pore former (PEG-400, 0.5, 1.5 and 2.5 % w/v) were dissolved in acetone and stored in a refrigerator until use. Coating solution CT-1 was composed from cellulose acetate (5 % w/v), 1 % w/v of plasticizer dibutyl phthalate and no pore former.

In coating solution CT-2, the percent of the plasticizer dibutyl phthalate was increased to 2 % w/v and no pore former. Coating solutions CT-3 to CT-5 were composed of 5 % w/v cellulose acetate and 2 % w/v of plasticizer dibutyl phthalate and 0.5, 1.5 and 2.5 % w/v pore former PEG-400, respectively.

Each core tablet formula was coated with each coating solutions as follows: the coating process was carried out on a batch of 50 tablets in a conventional laboratory coating pan (Scientific Instrument, India) having an outer diameter of 10 cm. Rotation speed was maintained at 20 rpm and hot air inlet temperature was kept at 38-40 °C.

The manual coating procedure based on intermittent spraying and coating procedure was used with spray rate of 3 mL/min. The coating process of the core tablets was continued until an increase of about 8 % in the tablet weight was obtained. In all cases, coated tablets were dried at 50 °C for 6 h before further evaluation.

A small orifice ranging from 250 to 350 μm was drilled through one side of each coated tablet by a standard mechanical microdrill.

3. Release rate studies of KT from the prepared osmotic pump tablets

The release of KT from the prepared tablets was performed using a dissolution tester apparatus 1 (Hanson Research, SR 8 plus model, Chatsworth, United States). Studies were carried out at 37 ± 0.5 °C in 900 mL of 0.1 N HCl for a period of 2 h followed by release in phosphate buffer pH 6.8 (0.2 M) for 10 h at rotation speed of 50 rpm. Five-milliliter samples were taken after 0.25, 0.5, 1, 2, 3, 4, 5, 6, 8, 10 and 12 h. The withdrawn samples were filtered through millipore filter (0.45 μm) and UV-analyzed for percent KT at 317 and 332 nm for 0.1 N HCl and phosphate buffer (pH 6.8), respectively. All experiments were carried out in triplicate (n = 3).

4. Kinetic analysis of the release data

To determine the mechanism of release of KT from its different OPTs, the release data was analyzed using linear regression according to:

$$\text{zero-order, } C_t = C_o - Kt$$

$$\text{first-order, } \text{Log } C_t = \text{Log } C_o - Kt/2.303$$

$$\text{simplified Higuchi diffusion model, } Q_t = K_H\, t^{0.5}$$

The correlation coefficient (R^2) was determined in each case and is used as a measure of release kinetics.

5. Effect of weight gain

To show the effect of weight gain after coating on the release of KT from the prepared osmotic pump tablets, coating process of OPT19

core tablets was continued until an increase in weight of about 6, 8 and 10 % was obtained. The release studies were performed on the new formulae in 900 mL of phosphate buffer pH 6.8 at a rotational speed of 50 rpm and 37 ± 0.5 °C. The experiments were carried out in triplicate (n = 3) and similarity factor (f2) was calculated for the release data to test similarity between the results.

6. Effect of agitation intensity

To show the effect of agitation intensity on the release of KT from the prepared osmotic pump tablets [28, 29], release studies on the optimized formulation were carried out in dissolution apparatus at various rotational speeds (50, 100 and 150 rpm). The results were the mean of triplicate (n = 3) and the significance of the difference between the results was evaluated by similarity factor (f2).

7. Effect of pH

To show the effect of pH on the release of KT from the prepared osmotic pump tablets, the optimized formula OPT19 was subjected to release studies in various media with different pH values. The media used were 0.1 N HCl (pH 1.2), phosphate buffer (pH 5.5) and phosphate buffer (pH 6.8) for 12 h and the % drug released was determined in each case. The difference between the results was evaluated by calculating the similarity factor (f2).

8. Effect of the type of coating polymer

To show the effect of the type of coating polymer on the release of KT from the prepared osmotic pump tablets, cellulose acetate propionate (average MN ~ 25,000) and cellulose acetate butyrate (average MN ~ 65,000) were used instead of cellulose acetate in coating solution (CT-4) and the new coating solutions were used in the preparation of OPT19.

The release studies on the new OPT19 formulae were carried out in dissolution apparatus under the same conditions mentioned previously in release rate studies. The similarity factor (f2) was used to show the difference between the results.

9. Scanning electron microscopy studies

In order to elucidate the mechanism of drug release from the developed formulae, coating membranes of formulation obtained before and after dissolution were examined for the porous morphology of their surfaces using a scanning electron microscope. After dissolution of 6 and 12 h, tablets were removed and dried at 40 °C for 12 h and then stored in desiccators until examination.

For the selected formula OPT19, both samples (before and after dissolution) were placed on a spherical brass stub with a double backed adhesive tape. The mounted samples were sputter coated with gold for 2 min using fine coat ion sputter (SPI sputter, United States) and then examined under a SEM (Joel JSM-6510LA, Japan) at a magnification power of 1000X and 2000X and an accelerating voltage of 20 kV.

III. RESULTS AND DISCUSSION

1. Drug excipient compatibility study

The compatibility of KT with the excipients used for formulation development was tested using differential scanning calorimetry (DSC) and IR spectroscopy.

DSC thermogram of plain KT shows a characteristic sharp endothermic melting peak at 169.62 °C. Thermograms for all KT excipient physical mixtures indicate that there was no appreciable shift in the melting peak of KT indicating no possible interaction between the drug and the tested excipients (*Figure 1*).

Concerning the IR spectrum of fresh KT, it is characterized by major bands in the functional group region at 3349.75 cm^{-1}, which is characteristic for (-OH) stretching vibration; the broadness of this band is indicative of hydrogen bonding. The strong band observed at 1557.24 cm^{-1} is attributable to the carbonyl (-C=O) stretching vibration.

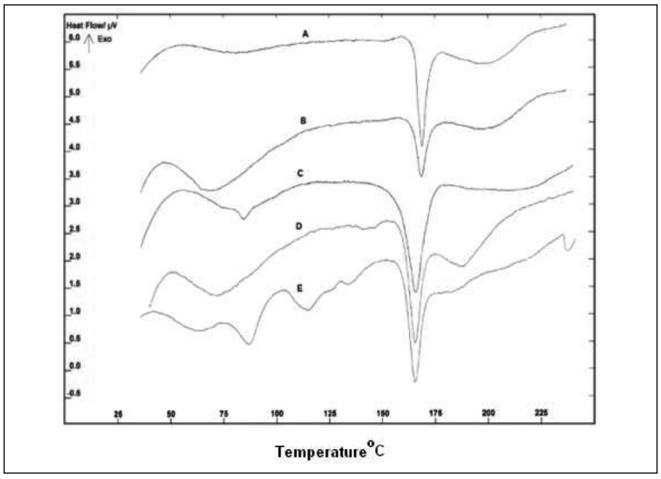

Figure 1 - DSC thermograms of (A) pure KT, (B) KT:NaCl, (C) KT:Compressol, (D) KT:cellulose acetate, (E) KT:Lubripharm SSF.

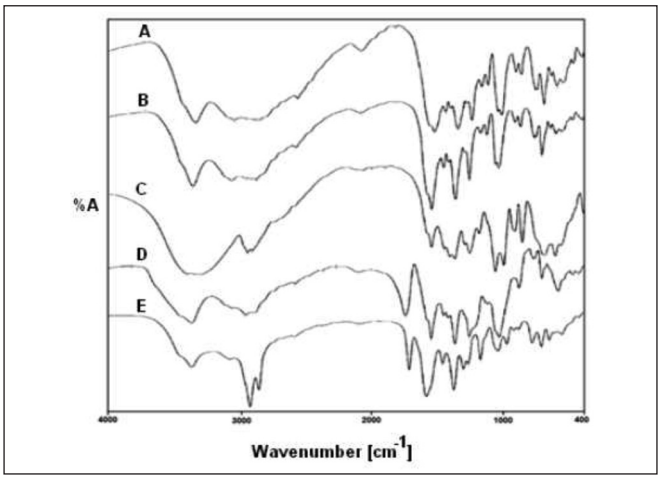

Figure 2 - IR spectra of (A) pure KT, (B) KT:NaCl, (C) KT:Compressol, (D) KT:cellulose acetate, (E) KT:Lubripharm SSF.

It is clear from the IR spectra of KT and its physical mixtures with excipients that the existence of the same characteristic bands of the drug and excipients in the same regions and at the same ranges may be with decreasing intensity in some cases due to dilution, and there are no new bands observed. This might be indicative of absence of any signs of chemical interaction between KT and the used excipients (*Figure 2*).

2. Characterization of the prepared core tablets

For the prepared core tablets CO1 to CO4, the following determinations were carried out: average weight, thickness, diameter and friability.

The average weight was in the range of 298 to 301 mg with S.D less than 0.089. The values of thickness and diameter fall in the range of 3.13 to 3.69 mm and 10.08 to 10.11 mm, respectively. All tablets showed percent of fines less than 0.24 indicating that they will be suitable for coating process and no roughness will appear in the formed coats.

3. Influence of formulation variables on KT release from osmotic pump tablets.

To study the influence of tablet formulation variables on drug release, four batches of core tablets with various formulation compositions were prepared; the percent of osmogent sodium chloride was increased from 0, 20, 40 to 60 % of the total tablet weight.

Table IV - Composition, increase in weight (%), thickness and diameter of different Ketorolac tromethamine osmotic pump tablets.

Formula	Composition	% increase in weight	Thickness (mm ± SD)	Diameter (mm ± SD)	Formula	Composition	% increase in weight	Thickness (mm ± SD)	Diameter (mm ± SD)
OPT1	CO-1/CT-1	7.95	3.93 ± 0.03	10.22 ± 0.02	OPT11	CO-3/CT-1	7.99	4.38 ± 0.07	10.23 ± 0.08
OPT2	CO-1/CT-2	7.89	3.88 ± 0.03	10.28 ± 0.02	OPT12	CO-3/CT-2	7.87	4.85 ± 0.18	10.25 ± 0.01
OPT3	CO-1/CT-3	8.12	4.15 ± 0.04	10.23 ± 0.01	OPT13	CO-3/CT-3	7.91	3.90 ± 0.04	10.21 ± 0.06
OPT4	CO-1/CT-4	8.29	4.20 ± 0.08	10.28 ± 0.03	OPT14	CO-3/CT-4	8.18	3.65 ± 0.04	10.28 ± 0.10
OPT5	CO-1/CT-5	7.92	3.80 ± 0.23	10.28 ± 0.01	OPT15	CO-3/CT-5	8.20	4.40 ± 0.04	10.27 ± 0.07
OPT6	CO-2/CT-1	7.91	3.95 ± 0.02	10.25 ± 0.01	OPT16	CO-4/CT-1	8.17	4.63 ± 0.03	10.27 ± 0.06
OPT7	CO-2/CT-2	8.45	4.11 ± 0.07	10.29 ± 0.01	OPT17	CO-4/CT-2	8.05	3.69 ± 0.02	10.20 ± 0.01
OPT8	CO-2/CT-3	8.08	4.21 ± 0.06	10.26 ± 0.03	OPT18	CO-4/CT-3	7.99	4.38 ± 0.07	10.23 ± 0.08
OPT9	CO-2/CT-4	8.34	3.95 ± 0.02	10.26 ± 0.06	OPT19	CO-4/CT-4	8.47	4.85 ± 0.18	10.25 ± 0.01
OPT10	CO-2/CT-5	8.05	3.69 ± 0.02	10.20 ± 0.01	OPT20	CO-4/CT-5	8.03	3.69 ± 0.02	10.29 ± 0.01

Plasticizer was used to modify not only the mechanical properties but also the thermal property, water absorption behavior and adhesive property of polymeric films. All of these properties affect the strength of coating films and the integrity of the final products, which further affect drug release performance [30, 31]. To study the effect of the plasticizer dibutyl phthalate, coating solutions CT-1 and CT-2 containing 1 and 2 % were prepared.

Water soluble polymers such as PVP, PEG and HPMC have been reported to leach out of the coating, forming a porous film with increased permeability, or produce hydrated water-filled HPMC regions within the membrane that allow drug transport across the film. It has been reported that PEG-400 is a better pore former than PVP and HPMC since it is a more hydrophilic plasticizer and can be leached out easily and increase the flux rate of fluid [32].

To study the effect of the level of pore former PEG-400, coating solutions (CT3-CT5) containing 0.5, 1.5 and 2.5 % w/v of PEG-400 were prepared. Twenty osmotic pump tablet formulae were obtained by coating each core tablet formula (CO1-CO4) with coating solutions of different compositions (CT1-CT5).

Table IV shows the % increase in weight, thickness and diameter of the prepared osmotic pump tablet formulae. Tablets show an increase in weight by 7.87 to 8.47 %.

The membrane is permeable to aqueous fluids but substantially impermeable to the components of the core. In operation, the core compartment imbibes aqueous fluids from the surrounding environment across the membrane and dissolves the drug. The dissolved drugs are released through the pores created after leaching of water-soluble additive(s) in the membrane.

Release profiles of KT from different osmotic pump tablet formulae OPT1-OPT5 are presented in *Figure 3A*. The percents of drug released after 1 h were 0.94, 0.29, 1.42, 2.36 and 4.78 %, respectively, while the percents of drug released after 6 h were 10.26, 6.91, 15.32, 29.84 and 49.42 %. After 12 h, the percents of drug released were 32.41, 20.03, 44.05, 67.14 and 75.75 %, respectively.

It is clear that drug release increased with the increase in the level of pore former. As the level of pore former increases, the membrane becomes more porous after coming in contact with the aqueous environment, resulting in faster drug release. Similar results are observed in a previous work [33, 34].

Concerning release profiles of KT from different osmotic pump tablet formulae OPT6-OPT10, the percents of drug released after 1 h were 0.38, 0.25, 1.37, 3.46 and 5.16 %, respectively while the percents of drug released after 6 h were 17.29, 7.23, 23.26, 35.50 and 48.31 %. After 12 h, the percents of drug released were 39.12, 25.06, 53.05, 69.30 and 75.80 %, respectively. All of these formulae contain 20 % sodium chloride in their cores, but no significant increase was attributed to the presence of this percent of sodium chloride (*Figure 3B*).

Formulae OPT11-OPT15 containing 40 % sodium chloride in their cores had different release profiles since the percents of drug released after 12 h were 47.00, 32.36, 62.76, 86.97 and 79.69 %, respectively (*Figure 3C*).

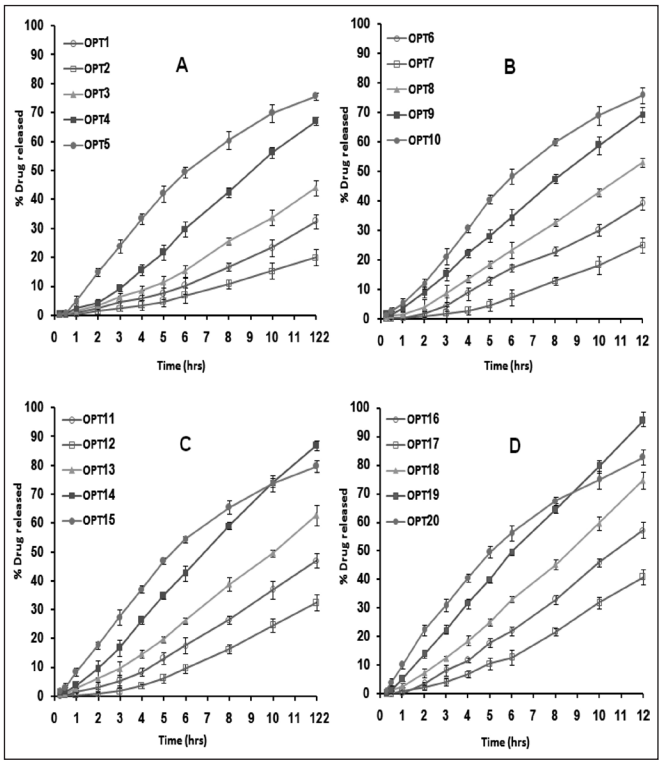

Figure 3 - Release profiles of KT from osmotic pump tablet formulae: (A) OPT1-OPT5, (B) OPT6-OPT10, (C) OPT11-OPT15 and (D) OPT16-OPT20.

As shown in *Figure 3D*, addition of 60 % of sodium chloride in the cores of osmotic pump tablets OPT16-OPT20 resulted in more of an increase in the drug released after 6 and 12 h. The drug release rate was fast and the lag time was short; this is due to this high percent of sodium chloride exerting a high osmotic pressure difference leading to an increase in the rate of medium permeation into the matrix of the core tablet. As a result, an increased internal pressure leads to a fast release rate.

Formula OPT19 showed the highest release rate: 5.22, 49.74 and 95.56 % of the labeled drug were released after 1, 6 and 12 h, respectively. This formulation was selected as the optimized formulation and used for further evaluation studies.

It was found that drug release from formulae OPT5, OPT10, OPT15 and OPT20 was higher and of a non-linear drug release profile. These formulae contain 50 % w/w of PEG-400 in their coatings. They develop a porous membrane on the surface of the core tablet and this in turn allows free diffusion of drug molecules along the concentration gradient, irrespective of the composition of the core tablets.

On the other hand, the presence of 2 % plasticizer dibutyl phthalate in the coating films plays role to countercurrent drug release. All OPT formulae containing 2 % plasticizer in their coats showed significant

decrease in drug release rate compared to those containing 1 % at the same composition of core tablets, since OPT1 > OPT2, OPT6 > OPT7, OPT11 > OPT12 and OPT16 > OPT17 in the percent drug release after 1, 6 and 12 h.

This observation could be explained by the presence of dibutyl phthalate at a higher concentration (2 % w/v) in the coating films resulting in more elasticity of the film so that the increase in the internal pressure is compensated by increase in the tablet dimensions due to the effect of elastic film, which slow down the release to some extent. In contrast, 1 % w/v dibutyl phthalate in the film does not offer the elasticity required to compensate the pressure, so an increase in increased internal pressure leads to faster drug release.

Concerning the lag time seen with tablets coated with CT-1, CT-2 and CT-3, it was reduced by using a hydrophilic substance, PEG-400, in combination with dibutylphthalate in concentrations larger than 10 % w/w (CT-4 and CT-5). As PEG-400 was a hydrophilic substance, it could be leached easily and left behind a porous structure, which enhanced the membrane permeability and drug release rate.

4. Kinetics and mechanism of drug release

Drug release data from the different formulations were fitted to various kinetic models to elucidate the mechanism and kinetics of drug release (kinetic data are shown in *Table V*).

According to regression constant (R^2) for the release data of most formulae, the most appropriate model was zero-order kinetics. The compatible fit of zero-order kinetics indicated that drug release is controlled by a concentration-independent release mechanism. Coating membranes in these formulae behaved like true semipermeable membranes, resulting in zero-order delivery of drug through the orifice only under the control of osmotic pressure gradient across the membrane.

Drug release from formulae OPT5, OPT10, OPT15 and OPT20 showed higher and non-linear drug release profiles (first-order release kinetics).

This observation could be explained on the basis that their coats contain the highest percent (50 %) of pore former PEG-400 and when they came in contact with the aqueous environment during the release study, the water soluble PEG-400 leached out leaving behind a highly porous membrane on the surface of the core tablet, which allowed free diffusion of drug molecules along the concentration gradient.

Table V - Kinetics data and release mechanism of ketorolac tromethamine from different OPTs.

Formula	Correlation coefficient (R^2) for			Release model
	Zero order	First order	Diffusion model	
OPT1	**0.9592**	0.9368	0.8431	**Zero**
OPT2	**0.9656**	0.9554	0.8502	**Zero**
OPT3	**0.9739**	0.9474	0.8678	**Zero**
OPT4	**0.9881**	0.9526	0.9022	**Zero**
OPT5	0.9700	**0.9982**	0.9866	First
OPT6	**0.9855**	0.9715	0.8982	**Zero**
OPT7	**0.9386**	0.9236	0.8025	**Zero**
OPT8	**0.9920**	0.9700	0.9114	**Zero**
OPT9	**0.9982**	0.9758	0.9462	**Zero**
OPT10	0.9780	**0.9944**	0.9744	First
OPT11	**0.9744**	0.9469	0.8666	**Zero**
OPT12	**0.9364**	0.9171	0.7972	**Zero**
OPT13	**0.9884**	0.9501	0.9005	**Zero**
OPT14	**0.9969**	0.9315	0.9391	**Zero**
OPT15	0.9628	**0.9981**	0.9882	First
OPT16	**0.9849**	0.9503	0.8904	**Zero**
OPT17	**0.9627**	0.9364	0.8452	**Zero**
OPT18	**0.9935**	0.9357	0.9154	**Zero**
OPT19	**0.9989**	0.8591	0.9607	**Zero**
OPT20	0.9587	**0.9988**	0.9950	First

These results were in accordance with Rani *et al*. whose work had focused on the preparation and evaluation of osmotic pump tablets for the controlled delivery of diclofenac sodium [35].

5. Effect of weight gain

The effect of increase in weight on the release of KT from the prepared osmotic pump tablets was studied on OPT19 core tablets after an increase in weight of 6, 8 and 10 %.

As shown in *Figure 4A*, KT release shows a difference in release profiles. The release from formulae with 6 and 10 % differs from release of formula with an 8 % increase in weight. The values of similarity factor (f2) were 49.61and 46.88 for formulae with an 8 and 10 % increase in weight, respectively, indicating no similarity between the two dissolution profiles, since the FDA has set a public standard of f2 value greater than 50 to indicate similarity between two dissolution profiles.

6. Effect of agitation intensity

The effect of agitation intensity of the release media on the release of KT from the selected formula OPT19 was carried out in USP dissolution apparatus type II at varying rotational speeds (50, 100 and150 rpm).

From *Figure 4B*, it is clear that the release of KT from the optimized formulation OPT19 is independent of the agitation intensity since the differences between the release data at 50, 100 and150 rpm is non-significant and values of similarity factor (f2) were 83.21 and 77.27 for release profiles at 100 and 150 rpm, respectively, indicating the high similarity between the two dissolution profiles and the dissolution profile at 50 rpm.

Hence, it can be expected that the release of KT from the developed formulation will be independent of the hydrodynamic conditions of the absorption site. Drug release from osmotic pumps to a large extent is independent of agitation intensity of the release media. These results comply with the results of the previously published work of Liu *et al*. [36].

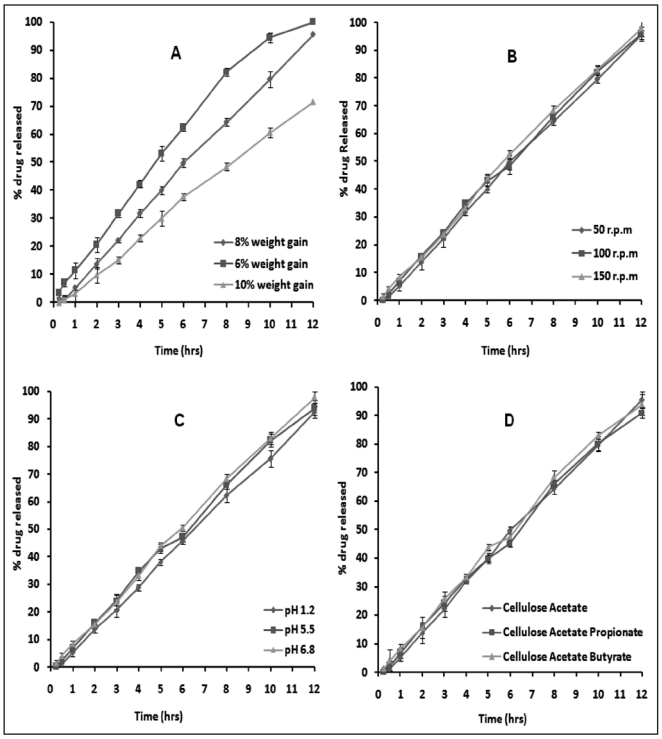

Figure 4 - Release profiles of KT from the selected formula OPT19 showing: (A) effect of increase in tablet weight after coating, (B) effect of agitation intensities, (C) effect of pH of release medium and (D) effect of coating polymer type.

7. Effect of pH of release medium

The effect of pH of release medium on drug release was conducted in media of different pH. There was similarity between the results of the release data in pH 1.2 and 5.5 since the values of similarity factor (f2) were 80.60 and 80.12, respectively.

As can be seen from *Figure 4C*, the release profiles being similar in all the media demonstrate that the developed formula OPT19 shows pH-independent release. These results were in accordance with the previously published work of Makhija *et al*. [8].

8. Effect of the type of coating polymer

The effect of the coating polymer type on the release of KT from the prepared osmotic pump tablet studied. From *Figure 4D*, it is obvious that the release of KT from the optimized formulation OPT19 is not affected by the type of polymer in the coating solution. The observed difference was non-significant where the f2 values were higher than 50.

Coating membranes made from cellulose acetate, cellulose acetate propionate and cellulose acetate butyrate had the same effect in controlling the release of KT from the prepared osmotic pump tablets.

9. Scanning electron microscopy studies

In order to investigate the changes in the membrane structure, the surface of coated tablets was studied using a scanning electron microscope. It was expected that with an increase in the level of pore former, the porosity of the membrane would increase because of leaching of pore former from the membrane.

Figure 5 shows the SEM micrograph of the membrane surfaces of the selected formula OPT19 before and after dissolution studies. Before dissolution, the coating membrane was intact without any cracks and some pores in the membrane were observed which may be the result of bubbles on the surface that dried during the coating process.

After dissolution studies, coating membranes were also intact without any cracks. However, there was formation of many pores in the membranes, which possibly acted as exit ports for the drug. The number of pores observed after 12 h was much more than that observed after 6 h and this could be explained on the basis of leaching of pore former from the membrane.

*

Controlled elementary osmotic pump tablets of KT with a zero-order release were successfully developed. The formulation parameters such as presence of plasticizer, concentrations of the osmotic agent, concentrations of the pore former and the type of coating polymer on the permeability and the release profile were studied. Drug release from the developed formulations was found to be dependent on the percent increase in weight after coating, but independent of pH and the agitation intensity of the release media, suggesting that the release will be fairly independent of pH and hydrodynamic conditions of the body.

Also, the release appeared to be independent of the type of cellulose acetate derivatives used as coating polymers. Membranes were found to develop porous surfaces after coming in contact with the aqueous environment; the number of pores depends on the initial concentration of pore former in the coating membrane.

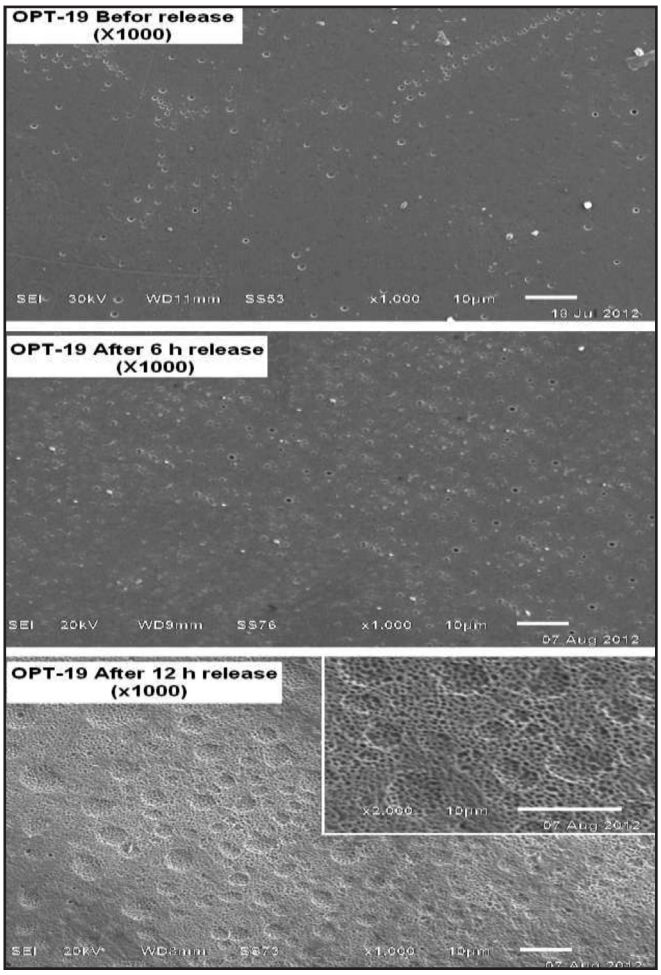

Figure 5 - SEM microphotographs of membrane surface of formula OPT19 before and after dissolution studies for 6 and 12 h.

REFERENCES

1. Amabile C.M, Bowman B.J. - Overview of oral modified-release opioid products for the management of chronic pain. - Ann. Pharmacother., **40** (7/8), 1327-1335, 2006.
2. Prisant L.M, Elliott W.J. - Drug delivery systems for treatment of systemic hypertension. - Clin. Pharmacokinet., **42** (11), 931-940, 2003.
3. Chien Y.W. - Novel Drug Delivery Systems. - 2nd ed., New York, Marcel Dekker, 2005, p. 139-196.
4. Liu H. - Chitosan-based controlled porosity osmotic pump for colon-specific delivery system: screening of formulation variables and *in vitro* investigation. - Int. J. Pharm., **332** (1), 115-124, 2007.
5. Tozaki H. - Chitosan capsules for colon-specific drug delivery: enhanced localization of 5-aminosalicylic acid in the large intestine accelerates healing of TNBS-induced colitis in rats. - J. Cont. Rel., **82** (1), 51-61, 2002.
6. Sharma S. - Osmotic controlled drug delivery system. - Latest Rev., **6**, 3, 2008.
7. Reza H., Vikram S.N., Kumaravelrajan R. - Formulation and optimization of aceclofenac monolith osmotic pump. - Int. J. Pharm. Sci. Rev. Res., **6**, 2, Article-010, 2011.
8. Makhija S.N., Vavia P.R. - Controlled porosity osmotic pump-based controlled release systems of pseudoephedrine. I. Cellulose acetate as a semipermeable membrane. - J. Cont. Rel., **89** (1), 5-18, 2003.
9. Verma R.K., Krishna D.M., Garg S. - Formulation aspects in the development of osmotically controlled oral drug delivery systems. - J. Cont. Rel., **79** (1), 7-27, 2002.
10. Kumar P., Singh S., Mishra B. - Development and evaluation of elementary osmotic pump of highly water soluble drug: tramadol hydrochloride. - Current Drug Delivery, **6**, 130-139, 2009.
11. Zhang Z.H., Dong H.Y., Peng B., Liu H.F., Li C.L., Liang M., Pan W.S. - Design of an expert system for the development and formulation of push-pull osmotic pump tablets containing poorly water-soluble drugs. - Int. J. Pharm., **410** (1-2), 41-47, 2011.
12. Patel V., Chudasama A., Nivsarkar M., Vasu K., Shishoo C.

- Push-pull osmotic pump for zero order delivery of lithium carbonate: development and *in vitro* characterization. - Pharm. Dev. Technol., **17** (3), 375-382, 2012. Epub 2011 Feb 2.
13. Patel A., Mehta T., Patel M., Patel K., Patel N. - Recent patent in controlled porosity osmotic pump. - Recent Pat. Drug Deliv. Formul., 2012 Aug 28.
14. Yakubu R., Peh K.K., Tan Y.T. - Design of a 24-hour controlled porosity osmotic pump system containing PVP: formulation variables. - Drug Dev. Ind. Pharm., **35** (12), 1430-1438, 2009.
15. Zulfequar A.K., Rahul T., Brahmeshwar M. - Floating elementary osmotic pump tablet (FEOPT) for controlled delivery of diethylcarbamazine. - AAPS PharmSciTech., **12** (4), 1312-1323, 2011.
16. Conley R., Gupta S.K., Sathyan G. - Clinical spectrum of the osmotic-controlled release oral delivery system (OROS), an advanced oral delivery form. - Curr. Med. Res. Opin., **22** (10), 1879-1892, 2006.
17. Kaushal A.M., Garg S. - An update on osmotic drug delivery patents. - Pharmaceutical Technology, 38-44, 2003.
18. Malaterre V., Ogorka J., Loggia N., Gurny R. - Oral osmotic driven systems: 30 years of development and clinical use. - Eur. J. Pharm. Biopharm., **73**, 311-323, 2009.
19. Prabakaran D. - Effect of hydrophilic polymers on the release of diltiazem hydrochloride from elementary osmotic pumps. - Int. J. Pharm., **259** (1), 173-179, 2003.
20. Thombre A. - Osmotic drug delivery using swellable-core technology. - J. Cont. Rel., 94 (1), 75-89, 2004.
21. Ghosh T., Ghosh A. - Drug delivery through osmotic systems – An overview. - J. App. Pharm. Sci., **1** (02), 38-49, 2011.
22. Verma R.K., Mishra B., Garg S. - Osmotically controlled oral drug delivery. - Drug Dev. Ind. Pharm., **26** (7), 695-708, 2000.
23. Verma R.K., Garg S. - Current status of drug delivery technologies and future direction. - Pharm. Tech., **25**, 1-14, 2001.
24. Rooks W. - The analgesic and anti-inflammatory profile of ketorolac and its tromethamine salt. - Drugs under Exp. Clin. Res., **11** (8), 479, 1985.
25. Buckley M.M, Brogden R.N. - Ketorolac: a review of pharmacodynamic and pharmacokinetic properties, and therapeutic potential. - Drugs, **39**, 86-109, 1990.
26. Reinhart D.I. - Minimizing the adverse effects of ketorolac. - Drug Safety, **22**, 487-497, 2000.
27. Bakan J. - The theory and Practice of Industrial Pharmacy. - Lea and Febiger, Philadelphia, 1986, p. 412-429.
28. Verma R.K., Garg S. - Development and evaluation of osmotically controlled oral drug delivery system of glipizide. - Eur. J. Pharm. Biopharm., **57** (3), 513-525, 2004.
29. Verma R.K., Kaushal A.M., Garg S. - Development and evaluation of extended release formulations of isosorbide mononitrate based on osmotic technology. - Int. J. Pharm., **263** (1), 9-24, 2003.
30. Lin W.J., Lee H.K., Wang D.M. - The influence of plasticizers on the release of theophylline from microporous controlled tablets. - J. Cont. Rel., **99**, 415-421, 2004.
31. Lin S.Y., Chen K.S., Run-Chu L. - Organic esters of plasticizers affecting the water absorption, adhesive property, glass transition temperature and plasticizer permanence of eudragit acrylic films. - J. Cont. Rel., 68, 343-350, 2000.
32. Rajagopal K., Nallaperumal N., Venkatesan S. - Development and evaluation of controlled porosity osmotic pump for Nifedipine and Metoprolol combination. - Lip. in Health Dis., **10**, 2011.
33. Garg A., Gupta M., Bhargava H. - Effect of formulation parameters on the release characteristics of propranolol from asymmetric membrane coated tablets. - Eur. J. Pharm. Biopharm., **67** (3), 725-731, 2007.
34. Liu L., Xu X. - Preparation of bilayer-core osmotic pump tablet by coating the indented core tablet. - Int. J. Pharm., **352** (1), 225-230, 2008.
35. Rani M. - Development and biopharmaceutical evaluation of osmotic pump tablets for controlled delivery of diclofenac sodium. - Acta Pharmaceutica-Zagreb, **53** (4), 263-274, 2003.
36. Liu L., Che B. - Preparation of monolithic osmotic pump system by coating the indented core tablet. - Eur. J. Pharm. Biopharm., 64 (2), 180-184, 2006.

ACKNOWLEDGMENTS

The authors wish to acknowledge El-Amerya pharmaceutical company (Egypt) for the gift sample of ketorolac tromethamine. Also, the authors are grateful to SPI Pharma (USA) for providing gift samples of Compressol SM and Lubripharm SSF.

DECLARATION OF INTEREST

The authors report no declarations of interest.

MANUSCRIPT

Received 30 October 2012, accepted for publication 18 December 2012.

International Journal of Pharmaceutics 471 (2014) 498–506

Contents lists available at ScienceDirect

International Journal of Pharmaceutics

journal homepage: www.elsevier.com/locate/ijpharm

Review

Oral transmucosal drug delivery – Current status and future prospects

Mohammed Sattar [a,b], Ossama M. Sayed [a,c], Majella E. Lane [a,*]

[a] Department of Pharmaceutics, UCL School of Pharmacy, 29-39 Brunswick Square, London WC1 N 1AX, United Kingdom
[b] Department of Pharmaceutics, College of Pharmacy, University of Basrah, Basrah, Iraq
[c] Pharmaceutics Department, Faculty of Pharmacy, Beni Suef University, P.O. Box 62514, Egypt

ARTICLE INFO

Article history:
Received 17 April 2014
Received in revised form 14 May 2014
Accepted 26 May 2014
Available online 29 May 2014

Keywords:
Oral transmucosal drug delivery
Buccal
Sublingual
Models
Formulations

ABSTRACT

Oral transmucosal drug delivery (OTDD) dosage forms have been available since the 1980s. In contrast to the number of actives currently delivered locally to the oral cavity, the number delivered as buccal or sublingual formulations remains relatively low. This is surprising in view of the advantages associated with OTDD, compared with conventional oral drug delivery. This review examines a number of aspects related to OTDD including the anatomy of the oral cavity, models currently used to study OTDD, as well as commercially available formulations and emerging technologies. The limitations of current methodologies to study OTDD are considered as well as recent publications and new approaches which have advanced our understanding of this route of drug delivery.

Contents

1. Introduction

Oral transmucosal drug delivery (OTDD) may be defined as the administration of pharmaceutically active agents through the oral mucosa to achieve systemic effects. This route has several advantages over conventional oral drug delivery as it avoids the

* Corresponding author. Tel.: +44 207 7535821; fax: +44 870 1659275.
E-mail address: majella.lane@btinternet.com (M.E. Lane).

http://dx.doi.org/10.1016/j.ijpharm.2014.05.043
0378-5173/

harsh acidic environment of the stomach and the enzymatic milieu of the small intestine. First pass hepatic metabolism is also circumvented if a molecule can penetrate the oral mucosa and attain therapeutic levels in the blood. The route should be distinguished from oral mucosal delivery (OMD) which aims to deliver drugs locally to the oral mucosal and which will be the subject of a forthcoming review.

The earliest record of OTDD appears to have been made by William Murrell, a licentiate of the Society of Apothecaries, who received his medical training at University College London. Murrell was one of the first scientists to report the clinical benefits from the administration of nitroglycerin drops in the management of patients afflicted with angina pectoris. An awareness of the importance of the actual route of administration is evident from the following:

> "Mr. Martindale kindly made me some pills composed of nitroglycerine dissolved in cocoa butter. They are perfectly active, but if swallowed in the ordinary way do not act so quickly as the spirituous solution."

(Murrell, 1882)

Despite this elementary demonstration of the efficacy of OTDD there was little development of buccal or sublingual dosage forms over the next 70–80 years. The seminal paper published in 1967, by Beckett and Triggs conclusively demonstrated that the loss of drug from a solution in the mouth could be attributed to oral mucosal absorption (Beckett and Triggs, 1967).

By the 1980s, the drugs registered in the US for administration via the buccal or sublingual routes included isosorbide dinitrate, ergot alkaloids, nicotine, testosterone and derivatives as well as nitroglycerine. Although the number of molecules administered via OTDD currently has expanded to include asenapine, buprenorphine, cannabis extracts, fentanyl, midazolam, naltrexone, prochlorperazine, selegiline and zolpidem this is still a relatively small category when compared with the transdermal route. The limited number of medicines on the market is surprising given the ever increasing interest in OTDD for paediatric and geriatric patients. The aims of this review are (i) to consider the physiological factors which limit OTDD (ii) to assess the models which have been used to study OTDD and (iii) to examine the different dosage forms currently available and (iv) to evaluate new technologies and strategies for OTDD.

2. Physiology of the oral mucosa

2.1. Buccal mucosa

The buccal mucosa delineates the inside lining of the cheek as well as the area between the gums and upper and lower lips and it has an average surface area of 100 cm^2. Its primary function is to protect underlying tissues from mechanical and chemical damage and the entry of foreign substances (Squier and Brogden, 2011). Structurally, it is a multilamellar lining consisting of the outer epithelium and basal laminar or basement membrane, supported by connective tissue consisting of the lamina propria and submucosa (Fig. 1). The undulating basement membrane is a continuous layer of extracellular material, approximately 1–2 μm in thickness. Mucus coats the surface of the epithelium and is discussed in more detail in Section 2.5.

The buccal epithelium is a non-keratinised stratified squamous tissue consisting of 40–50 layers of cells resulting in an overall thickness of 500–600 μm (Gandhi and Robinson, 1994). In the lower layers, cells are mitotically active and differentiate into larger and flatter cells as they approach the outer epithelium. The stages of this process are represented in four morphological layers, namely the basal layer, the prickle cell layer, the intermediate layer and the superficial layer. Membrane coating granules (MCGs) are first evident in the prickle cell layer. These granules fuse with the plasma membrane and extrude the lipid contents into the intercellular space in the outer third of the buccal epithelium. This outer area contains large amounts of phospholipids and relatively small amounts of ceramide. This is in contrast to stratum corneum where ceramides are one of the major lipid classes and which contains no phospholipids.

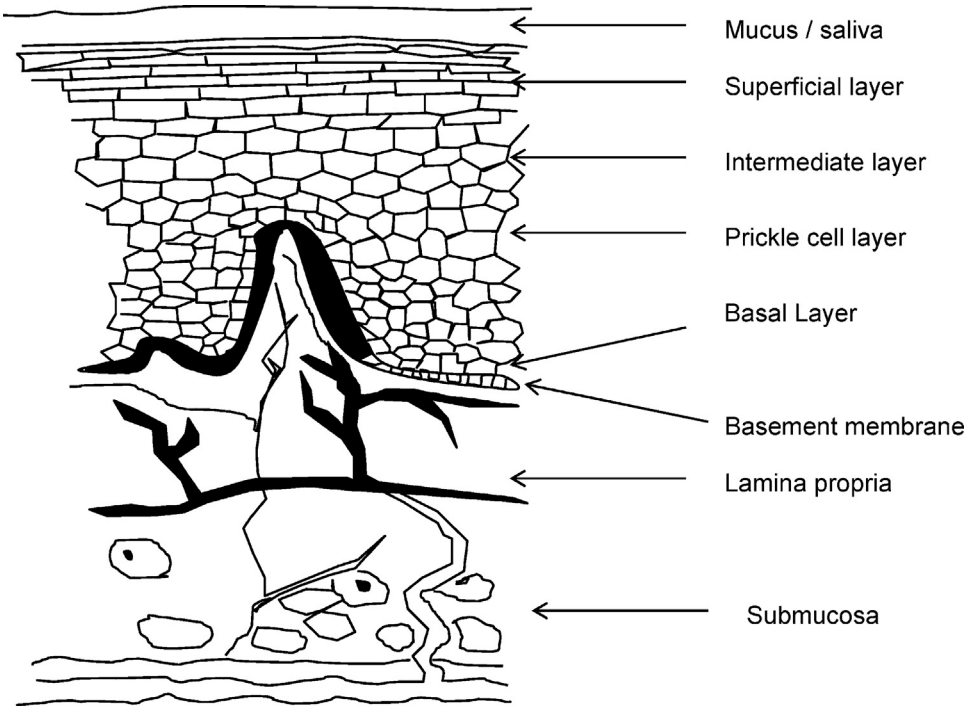

Fig. 1. Structure of buccal mucosa (adapted from Harris and Robinson, 1992).

The turnover time of buccal epithelial cells is 5–7 days. Secretory organelles extrude their lipid contents into the intercellular spaces about two thirds of the way from the basal layer to the surface which provides the major the barrier function of the epithelium (Dawson et al., 2013). The basal layer is approximately 1–2 μm thick and has also been suggested to contribute to the barrier properties of the mucosa (Harris and Robinson, 1992). The lamina propria is a loose, hydrated connective tissue composed of fibres of collagen with smooth muscles and capillaries and shows no significant effect on drug permeation (Veuillez et al., 2001). The submucosa consists of comparatively denser connective tissue with some accessory salivary glands surrounded by myoepithelial cells (Young et al., 2006). The blood flow to the buccal mucosa is of the order of 2.4 ml min^{-1} cm^{-2}.

2.2. Sublingual mucosa

Structurally the sublingual mucosa is comparable to the buccal mucosa but the thickness of this epithelium is 100–200 μm. This membrane is also non-keratinised and being relatively thinner has been demonstrated to be more permeable than buccal mucosa with respect to isosorbide dinitrate (Pimlott and Addy, 1985) as well as other molecules (Squier, 1991). Blood flow to the sublingual mucosal is slower compared with the buccal mucosa and is of the order of 1.0 ml min^{-1} cm^{-2}.

2.3. Gingival and palatal tissues

The gingival and palatal epithelia are keratinised with the former having a thickness of approximately 250 μm and the latter having a thickness of about 200 μm (Squier et al., 1976). These membranes are less permeable than the buccal and sublingual areas (Squier, 1991) but there are comparatively fewer published studies available for gingiva and hard palate compared with the other regions of the oral mucosa. As for the buccal mucosa, the keratinised regions also contain MCGs and the lipids present are acylceramides or ceramides (Squier, 1991).

2.4. Saliva

Saliva is a moderately viscous aqueous fluid secreted by parotid, submandibular, sublingual glands and minor salivary glands in the submucosa (Herrera et al., 1988). It functions as a lubricant, protective material, assists food mastication, prevents teeth demineralization, participates in carbohydrate metabolism and modulates the growth of oral flora (Slomiany et al., 1996). The major components of saliva are mucus (see Section 2.5), proteins, mineral salts, and enzymes. It is considered to be a weak buffer system with a pH of about 5.5–7. The pH range depends on ionic composition and flow rates. The ionic composition and flow rates of saliva are affected by type and degree of stimulation (smell, taste, and type of food) and time of the day. The normal salivary flow rate is approximately 0.5 ml/min resulting in total daily secretion between 0.5 and 2 l but due to continuous swallowing, the constant volume of saliva in the mouth is ~1.1 ml (Gilles and Ghazali, 1996).

2.5. Mucus

Mucus is an intercellular ground material secreted as a constituent of saliva from major and minor salivary glands. It is composed mainly of glycoproteins called mucins (Tabak et al., 1982) which are large molecules with a molecular weight from 0.5 to 20 MDa. Slomiany et al. (1996) have reviewed the molecular aspects of salivary mucins and the nature of the oral mucosa–mucin interactions. The negative charge of mucins at physiological pH values arises from the presence of sulphate and sialic acid residues. This negative charge allows mucin to bind to the surface of epithelial cells forming a gelatinous layer but a receptor for salivary mucins was also identified and characterized in buccal mucosa (Slomiany et al., 1993). Drug diffusion may be limited by the physical barrier of the mucus layer and also the specific or nonspecific binding of drugs to the mucus layer.

3. Permeation pathways and predictive models for OTDD

In general, the permeability of the oral mucosal epithelium is intermediate between that of the skin and the gut (Squier, 1991). Studies with tracer molecules, including horseradish peroxidase and lanthanum nitrate, have been conducted in rabbit and porcine models (Squier and Rooney, 1976; Squier and Hall, 1985) and indicate that the functional permeability barrier of the oral mucosa, like that of skin, is located in the epithelium and occupies the superficial layers. Other mechanistic studies to investigate drug transport in the buccal epithelium have been reported by Lesch et al. (1989); Hoogstraate et al. (1994); Nicolazzo et al. (2003, 2005). Although active transport processes have been investigated (Kurosaki et al., 1992, 1998) they do not appear to play a major role in OTDD. Structurally, the buccal and sublingual epithaliae essentially consist of cells embedded in an intercellular substance largely composed of carbohydrate–protein complexes. Two routes of drug transport are generally proposed: paracellular (between the cells) and transcellular (across the cells). Some researchers have suggested that hydrophilic molecules will permeate via the paracellular route while lipophilic molecules will be absorbed preferentially via the transcellular route (Zhang and Robinson, 1996; Deneer et al., 2002).

Kokate et al. (2008a) investigated the contribution of thermodynamic activities of ionized and unionized species on buccal drug permeation using nimesulide and bupivacaine as model drugs. In vitro studies were conducted with porcine tissue and horizontal side-by-side cells. For nimesulide saturated or subsaturated buffered drug solutions were applied to the donor chamber at different pH values ranging from 5.0 to 8.0. Saturated and subsaturated buffered solutions of bupivacaine were investigated in the pH range 6.0–8.5. The receptor chamber contained buffer at the same pH as the respective donor solutions. The thermodynamic activities of ionized and unionized drug species were expressed as degree of saturation (DS) and were also calculated using a modified Debye–Hückel equation. For both drugs, the permeability of the ionized species was approximately fourfold lower than the unionized species. Assuming that both the ionized and unionized species contribute independently to the total steady-state flux theoretical estimations were made for total drug flux values and percent contribution of the ionized species to the total flux. The contribution of the ionized species to total flux was estimated to be equal to that of the unionized species when 90% of the drug was in the ionized state.

Goswami et al. (2009) used polyethylene glycols as model hydrophilic permeants to establish theoretical pore sizes for permeation of hydrophilic molecules across the different regions of the oral mucosa. Permeation studies were carried out in vitro with porcine buccal tissue for a period of 8 h to a maximum of 12 h to obtain the steady-state flux values for PEG oligomers with different molecular weights. PEG solutions with mean molecular weights of 300, 400, 600, 1000 (5%, w/v) were prepared by dissolving appropriate amount of PEG in isotonic phosphate buffer solution (pH 7.4). Experimentally determined permeability and theoretical diffusion parameters for PEG molecules were used to calculate the radius of the pore (r_p) for the aqueous pathways in buccal and sublingual tissues as 18–22 and 30–53 Å, respectively. The authors further noted that the presence of this aqueous route

might explain the significant contribution of the ionized species of a drug to the total flux across the oral mucosa observed by Kokate et al. (2008a).

Kokate et al. (2008b) also reported the in vitro flux values of a larger group of drugs, namely three acidic (naproxen, warfarin, nimesulide), seven basic (lidocaine, propranolol, verapamil, diltiazem, amitriptyline, metoprolol, pindolol), and two neutral (caffeine, antipyrine) molecules across porcine buccal mucosa. Values for log P and $\log_{10}$ of distribution coefficient (log D) at pH 6.8, which corresponds to salivary pH values were obtained either from the literature or were estimated using National Institutes for Health ChemIDplus software. For drugs with poor solubility (diltiazem, amitriptyline, nimesulide, naproxen, warfarin), saturated donor drug solutions were used. The initial drug concentration for the remaining drugs was 1.0 mg/ml (verapamil), 5.0 mg/ml (lidocaine, propranolol, caffeine, antipyrine), 7.5 mg/ml (metoprolol) and 10 mg/ml (pindolol). When permeability coefficients were plotted against log P a poor correlation was obtained ($r^2 = 0.53$); however, the correlation improved significantly when log $D_{6.8}$ was plotted instead of log P ($r^2 = 0.73$).

In a later study (Kokate et al., 2009), the apparent permeability coefficients of 15 different drugs across porcine buccal mucosa were used to develop an in silico model predictive of buccal permeation. Multiple linear regression (MLR) and maximum likelihood estimations (MLE) were used to develop the model based on permeability as the response variable and various descriptors as the predictor variables. The various descriptors used were molecular weight (MW), molecular volume (MV), octanol–water partition coefficient (log P), log $D_{6.8}$ (logarithm of distribution coefficient at pH 6.8, which corresponds to salivary pH), polar surface area (TPSA), number of hydrogen bond acceptors (HBA) and donors (HBD), number of rotatable bonds (nRotB), solubility (at pH 6.8), and melting point (mp). Four descriptors, MV, log $D_{6.8}$, HBD, and nRotB, were found to influence permeability significantly. The final model was validated with an external data set consisting of permeability values obtained for 12 drugs from the literature. Using a similar approach with 14 model drugs, an in silico model was developed to predict sublingual permeability (Goswami et al., 2013). MLR analysis indicated that HBD and log $D_{6.8}$ were the significant descriptors. When compared with the buccal in silico model the authors proposed that the absence of nRotB and MV in the sublingual model reflected differences in the physiological and biochemical properties of the two mucosae.

Amores et al. (2014) determined the apparent permeability coefficient, (k_p) flux (J) and lag time, T_L of a series of β-blockers (acebutolol, atenolol, labetalol, metoprolol, oxprenolol and propranolol) through porcine buccal mucosa. MLR using least square estimation was performed on the data set with log k_p as the dependent variable and solubility, MW, MV, TPSA, HBA, HBDm and nRotB as the predictor variables. Stepwise regression and MLR analysis resulted in the following model:

$$\log k_p(\mathrm{cm/h}) = -3.885(\pm 3.770) + 1.626(\pm 0.625) \times \log D_{\mathrm{pH6.8}} - 0.521(\pm 0.297) \times \mathrm{nRotB} + 2.236(\pm 1.023) \times \mathrm{HBA}$$

Regression analysis showed that 85.7% of variability in permeability data could be explained by the model.

4. Models to study OTDD

4.1. Studies in man and human tissue models

The oral absorption test, also known as the 'swirl and spit' test, was developed by Beckett and Triggs (1967). It involves swirling a known volume of a specific drug concentration for a fixed period of time by human volunteers followed by expulsion of the solution. The volunteers then rinse their mouth with a known volume of buffer solution and the expelled drug solution and the rinse are combined and analysed for drug content. The absorbed amount of drug is assumed to be the difference between the initial and final drug concentration in the solution. A series of papers from Beckett's laboratory in the 1960s and 1970s used this model to demonstrate the buccal absorption of different drugs and the influence of pH on the absorption of a range of drugs (Beckett and Moffat, 1968, 1969a,b, 1970, 1971; Beckett and Pickup, 1975). The limitations of this method include (i) the possible dilution of the drug solution by continuous salivary production, which is stimulated by swirling and (ii) unintentional swallowing. Non-absorbable markers have been used to account for salivary secretion and swallowing (Tucker, 1988). A further problem is that absorption takes place from all regions of the oral cavity, with no control over the area across which absorption can take place. Finally, disappearance from the oral cavity is not necessarily an indication of complete transfer to the systemic circulation because of potential metabolism and/or tissue binding.

The use of perfusion cells in the oral cavity was developed to overcome some of the limitations of the original oral absorption method. Drug transfer takes place over an isolated area and interference from salivary secretions is prevented; volume, pH and temperature of the perfusant are also maintained constant (Rathbone, 1991). This model has been used to study human buccal absorption of nicotine by Adrian et al. (2006). These workers also examined parotid saliva for nicotine levels but a correlation between saliva and plasma levels for oral transmucosal delivery has yet to be established.

Recently, Pudney et al. (2012) have reported a new in vivo Raman probe that allows depth profiling of the buccal epithelium. A small external optical window is set at the end of a long pen-shaped device, which can be maneuvered against the buccal epithelium, with minimal discomfort to the subject. Within this pen-shaped probe is a small objective, 12 mm in diameter which is moved backwards and forwards by a motor to change the location of the laser focus in the tissue. This probe is attached to an in vivo Raman spectrometer with three exit ports one of which directs the laser beam into the probe. As with the main spectrometer, the fingerprint region is measured using 785 nm excitation and the high wavenumber region is measured using 671 nm excitation. Measurements of the oral mucosa were carried out in 2 subjects by placing the probe inside the mouth on the cheek and depth scans were taken. The mouth was then rinsed with solutions (0.0183%, 0.183%, or 1.83% by weight) of epigallocatechin gallate (ECG). The ECG signal was observed clearly in the buccal epithelium and was still present after 15 min exposure for the 0.183% solution. The ability to probe the buccal epithelium at the molecular level with confocal Raman spectroscopy should facilitate a better understanding of the barrier properties of this tissue. Monitoring of actives may be possible where the molecule has a suitable Raman spectrum.

In vitro studies with human biopsy or cadaver tissue are sparse in the literature but these models have been used by Nielsen and Rassing (2000) to study buccal permeation of β-blockers and testosterone and by van der Bijl et al. (2000) to study sumatriptan.

4.2. Porcine models

Porcine oral mucosal tissue has similar histological characteristics to human oral mucosal tissue (Heaney and Jones, 1978; Collins et al., 1981). Lesch et al. (1989) reported that the water permeability of porcine buccal mucosa was not significantly different from human buccal mucosa but the floor of the mouth was more permeable in human tissue than in pig tissue. Comparisons between fresh porcine tissue specimens and those stored at −80 °C also revealed no significant effect on permeability

as a result of freezing. Porcine buccal mucosal absorption has been studied for a wide range of drug molecules both in vitro and in vivo (Table 1). Typically, in vitro studies involve mounting excised porcine buccal tissue in Ussing chambers, Franz cells or similar diffusion apparatus. The in vivo studies described in the literature involve the application of the drug as a solution, gel or device to the buccal mucosa of pigs followed by plasma sampling.

Nicolazzo et al. (2003) investigated the effects of various in vitro conditions on the permeability of porcine buccal tissue using caffeine and oestradiol as model hydrophilic and lipophilic marker molecules. Drug permeation in the buccal mucosa was studied using modified Ussing chambers. Comparative permeation studies were performed through full thickness and epithelial tissues, fresh and frozen tissues. Tissue integrity was monitored by the

Table 1
Drugs studied with porcine models for oral transmucosal drug delivery.

Drug	Type of study	Authors
(D-ala2, D-leu5)-enkephalin	In vitro	Lee and Kellaway (2000)
(D-Pen2, D-Pen5)-enkephalin	In vitro	Yuan et al. (2011)
5-aza-2-deoxycytidine	In vitro	Mahalingam et al. (2007)
Acyclovir	In vitro	Shojaei et al., (1998)
Antipyrine	In vitro	Kulkarni et al. (2011)
Atenolol HCl	In vitro	Jacobsen (2001)
Bupivacaine	In vitro	Kulkarni et al. (2011)
Buserelin	In vivo	Hoogstraate et al. (1996)
Buspirone	In vitro	Birudaraj et al. (2005)
Caffeine	In vitro	Nicolazzo et al. (2004)
Calcitonin (salmon)	In vitro	Oh et al. (2011)
Carbamazepine	In vitro	Giannola et al. (2005)
Carvedilol	In vitro	Cappello et al. (2006)
Celecoxib	In vitro	Cid et al. (2012)
Chlorpheniramine maleate	In vitro	Sekhar et al. (2008)
Diazepam	In vitro	Meng-Lund et al. (2014)
Diclofenac sodium	In vitro	Miro et al. (2009)
Didanosine	In vitro	Ojewole et al. (2012)
Dideoxycytidine	In vitro	Shojaei et al., (1999)
Diltiazem hydrochloride	In vitro	Hu et al. (2011)
Domperidone	In vitro	Palem et al. (2011b)
Donazepil hydrochloride	In vitro	Caon et al. (2014)
Endomorphin-1	In vitro	Bird et al. (2001)
Felodipine	In vitro	Palem et al. (2011a)
Fentanyl	In vitro	Diaz Del Consuelo et al. (2005)
Flecainide	In vitro	Deneer et al. (2002)
Galantamine hydrobromide	In vitro	De Caro et al. (2008)
	In vivo	Giannola et al. (2010)
Insulin	In vitro	Das et al. (2012)
Lamotrigine	In vitro	Mashru et al. (2005b)
Lercanidipine hydrochloride	In vitro	Charde et al. (2008)
Methimazole	In vitro	De Caro et al. (2012)
Metoprolol	In vitro	Nielsen and Rassing (2000)
	In vivo	Holm et al. (2013)
Morphine hydrochloride	In vitro	Senel et al. (1998)
Naltrexone hydrochloride	In vitro	Giannola et al. (2007)
	In vivo	Campisi et al. (2010)
Nicotine	In vitro	Nair et al. (1997)
Nicotine hydrogen tartrate	In vitro	Hu et al. (2011)
Nimesulide sodium	In vitro	Maffei et al. (2004)
Nortestosterone	In vivo	Claus et al. (2007)
Oestradiol	In vitro	Nicolazzo et al. (2004)
	In vivo	Claus et al. (2007)
Omeprazole	In vitro	Figueiras et al. (2009)
Ondansetron hydrochloride	In vitro	Mashru et al. (2005a)
Phenylephrine	In vitro	Rao et al. (2011)
Phenytoin sodium	In vitro	Adeleke et al. (2010)
Pioglitazone	In vitro	Palem et al. (2011a)
Pituitary adenylate cyclase-activating polypeptide	In vitro	Langoth et al. (2005)
Pravastatin sodium	In vitro	Shidhaye et al. (2010)
Progesterone	In vitro	Jain et al. (2008)
Propranol HCl	In vitro	Lee and Choi (2003)
Risperidone	In vitro	Heemstra et al. (2010)
Rizatriptan benzoate	In vitro	Avachat et al. (2013)
Ropinirole	In vitro	De Caro et al. (2012)
Salbutamol sulphate	In vitro	Puratchikody et al. (2011)
Saquinavir	In vitro	Rambharose et al. (2014a)
Sotalol	In vitro	Deneer et al. (2002)
Sumatriptan succinate	In vitro	Prasanna et al. (2011)
Tacrine	In vitro	Gore et al. (1998)
Tenofovir	In vitro	Rambharose et al. (2014b)
Testosterone	In vitro	Nielsen and Rassing (2000)
	In vivo	Claus et al. (2007)
Thiocolchicoside	In vitro	Artusi et al. (2003)
Transforming growth factor-beta	In vitro	Senel et al. (2000)

absorption of the fluorescein isothiocyanate (FITC)-labeled dextran 20 kDa (FD20) and tissue viability was assessed using an MTT (3-[4,5-dimethylthiazol-2-yl]-2,5-diphenyltetrazolium bromide) biochemical assay and histological evaluation. Permeability through the buccal epithelium was 1.8-fold greater for caffeine and 16.7-fold greater for oestradiol compared with full thickness buccal tissue. Flux values for both compounds were comparable for fresh and frozen buccal epithelium although histological evaluation demonstrated signs of cellular death in frozen tissue. The tissue appeared to remain viable for up to 12 h postmortem using the MTT viability assay which was also confirmed by histological evaluation.

Kulkarni et al. (2009) investigated the relative contributions of the epithelium and connective tissue to the barrier properties of porcine buccal tissue. In vitro permeation studies were conducted with antipyrine, buspirone, bupivacaine and caffeine as model permeants. The permeability of the model diffusants across buccal mucosa with thickness of 250, 400, 500, 600, and 700 μm was determined. A bilayer membrane model was developed to delineate the relative contribution to the barrier function of the epithelium and the connective tissue. The relative contribution of the connective tissue region as a permeability barrier significantly increased with increasing mucosal tissue thickness. A mucosal tissue thickness of ~500 μm was recommended by the authors for in vitro transbuccal permeation studies as the epithelium represented the major permeability barrier for all diffusants at this thickness. The authors also investigated the effects of a number of biological and experimental variables on the permeability of the same group of model permeants in porcine buccal mucosa (Kulkarni et al., 2010). Significantly, higher permeability of the permeants was observed for the thinner region behind the lip (170–220 μm) compared with the thicker cheek (250–280 μm) region. Porcine buccal mucosa retained its integrity in Kreb's bicarbonate ringer solution at 4 °C for 24 h. Heat treatment to separate the epithelium from underlying connective tissue did not adversely affect its permeability and integrity characteristics compared with surgical separation.

4.3. Dog, monkey and rabbit models

In vivo studies have been conducted with both dogs and monkeys as the buccal epithelium is non-keratinised in these species. However, higher permeability has been reported in these models for tritiated water compared with human tissue, presumably because of the relatively thinner buccal epithelia in these animals (Squier and Wertz, 1996). The rabbit buccal mucosa is partially non-keratinised and has proved a popular model to study buccal drug delivery over the years, in both in vitro and in vivo studies. However, difficulties in isolating non-keratinised tissue from keratinised tissue in rabbits have been highlighted by Squier and Wertz (1996).

4.4. Chicken, hamster and rat models

Although chicken pouch membranes have been used to evaluate buccal drug delivery in vitro by a number of researchers, there is no evidence to suggest that this is a suitable model membrane for predicting buccal delivery in humans (El-Samaligy et al., 2004; Kamel et al., 2012). Rat oral cavity and hamster cheek pouch are keratinised so are not appropriate models when developing or screening formulations for administration to humans. Notwithstanding this limitation there are many studies in the literature which have used such tissues.

4.5. Cell culture models

The TR 146 cell line originated from a squamous cell carcinoma of the buccal mucosa (Rupniak et al., 1985) and was originally developed as an in vitro model of the buccal mucosa by Rassing and co-workers (Jacobsen et al., 1999; Nielsen et al., 1999). However, the barrier function of this model was reported to be lower than porcine or human buccal tissue (Nielsen and Rassing, 2000). Correlations for in vitro studies conducted with porcine buccal tissue and the TR 146 model have been proposed for nicotine (Nielsen and Rassing, 2002). Recently the permeability of metoprolol was demonstrated to be similar in both TR 146 studies and porcine buccal tissue; an in vitro–in vivo correlation was also proposed based on studies conducted in minipigs (Holm et al., 2013). A human tumour cell line established from human sublingual squamous cell carcinoma was investigated by Wang and colleagues (Wang et al., 2007, 2009) as an in vitro model of the sublingual mucosa. Based on studies with a number of beta blockers, the permeability characteristics of this cell line do not appear to mimic those of porcine sublingual tissue. EpiOral™ is a three-dimensional tissue culture model derived from healthy human buccal keratinocytes. Rao et al. (2011) reported similar permeability parameters for naltrexone hydrochloride using this model and porcine buccal tissue. However, unpublished data from our laboratory for domperidone permeation from simple solvents (Table 2) indicate that this model is more permeable than porcine buccal tissue. Saturated solutions of domperidone were applied either to porcine tissue or to EpiOral tissue mounted in vertical Franz cells. Studies were conducted for 8 h at 37 °C.

5. OTDD dosage forms

5.1. Commercially available dosage forms

Examples of commercially available OTDD products are provided in Table 3. Buccal and sublingual tablets are formulated using conventional tableting excipients such as buffering agents, diluents, disintegrants and sweeteners. Effentora® is an effervescent tablet. Some formulations also contain mucoadhesive polymers such as hypromellose and polycarbophil (e.g. Striant®). Fast acting disintegrants such as croscarmellose sodium and sodium starch glycolate are also used in Abstral® and Effentora®.

Buccolam® is a simple buffered aqueous solution of midazolam hydrochloride. Spray formulations such as Nitrolingual® contain ethanol as well as buffers, flavouring agents and solvents such as propylene glycol; a propellant is also included in Glytrin® (1,1,1,2-tetrafluoroethane). Chewing gum formulations of nicotine have been available for many years and the Nicorette® formulation contains a nicotine poloacrilin complex, as well as flavouring agents, sweeteners and other excipients.

Onsolis® (marketed as Breakyl® in Europe) is a soluble bilayer adhesive thin film formulation of fentanyl citrate which is applied to the buccal mucosa. The polymers used to prepare the active layer are carmellose sodium, hydroxyethyl cellulose, hydroxyl

Table 2
Comparison of domperidone permeability in porcine buccal mucosa and EpiOral™.

Solvent	Flux ($\mu g\,cm^{-2}\,min^{-1}$) $\times 10^2$ porcine buccal mucosa	k_p ($cm\,min^{-1}$) $\times 10^6$ porcine buccal mucosa	Flux ($\mu g\,cm^{-2}\,min^{-1}$) $\times 10^2$ EpiOral™	k_p ($cm\,min^{-1}$) $\times 10^6$ EpiOral™
PEG 200	1.4 ± 0.1	1.91 ± 0.18	6.2 ± 0.5	8.38 ± 0.68
PEG 400	1.2 ± 0.2	1.58 ± 0.34	2.3 ± 0.1	2.90 ± 0.10
Transcutol p™	7.4 ± 0.1	3.23 ± 0.52	20.7 ± 0.9	9.04 ± 0.37

Table 3
Examples of commercial oral transmucosal dosage forms.

Drug	Brand name and manufacturer	Dosage form and strength
Asenapine maleate	Sycrest® (Lundbeck)	Sublingual tablets; 5, 10 mg
Buprenorphine hydrochloride	Subutex® (Reckitt Benckiser)	Sublingual tablets; 400 μg, 2, 8 mg
Buprenorphine hydrochloride Naloxone hydrochloride dihydrate	Suboxone® (Reckitt Benckiser)	Sublingual tablet; 2 mg/500 mcg and 8 mg/2 mg Sublingual film; 2 mg/0.5 mg, 4 mg/1 mg, 8 mg/2 mg, 12 mg/3 mg
Delta-9-tetrahydrocannabinol cannabidiol (as extracts of *Cannabis sativa* L., Folium cum flore)	Sativex® (GW Pharma)	Oramucosal spray; Each 100 μl spray contains: 2.7 mg delta-9-tetrahydrocannabinol and 2.5 mg cannabidiol
Fentanyl citrate	Abstral® (ProStrakan)	Sublingual tablet; 100, 300, 600 mcg
	Actiq® (Cephalon)	Lozenge; 0.4, 0.6, 0.8, 1.2 mg
	Effentora® (Cephalon)	Tablets; 0.1, 0.2, 0.4, 0.6 and 0.8 mg
	Onsolis®	Soluble film; 200, 400, 800 mcg
Glyceryl trinitrate	Glytrin® (Sanofi)	Aerosol spray; 400 mcg/metered dose
	Nitrolingual® (Merck Serono)	Aerosol spray; 400 mcg/metered dose
Midazolam hydrochloride	Buccolam® (ViroPharma)	Oramucosal solution; 2.5, 5, 7.5, 10 mg
Nicotine	Nicorette®	Gum (nicotine resinate); 2, 4 mg Lozenge (nicotine resinate or nicotine bihydrogen tartrate); 2, 4 mg Oramucosal spray; 1 mg nicotine per spray dose Sublingual tablet (nicotinebitartrate); 2 mg
Prochlorperazine maleate	Buccastem M® (Alliance Pharmaceuticals)	Tablets; 3 mg
Testosterone	Striant® (Columbia Laboratories)	Tablets; 30 mg

propyl cellulose and polycarbophil. The drug free backing layer limits the exposure of the drug to saliva. Suboxone® contains buprenorphine HCl and naloxone HCl dihydrate in a hydroxypropyl methycellulose based film. Thin film formulation technology (TFT) is discussed further below.

5.2. Novel and emerging OTDD dosage forms

Although TFT appears to be an ideal delivery platform for buccal or sublingual delivery, only a limited number of APIs is available as OTDD dosage forms at present. A nanoparticle based formulation of insulin incorporated in film technology has been evaluated in Phase 1 trials by Midatech (www.midatech.com). From positive Phase I clinical trial results, it was reported that the transbuccal insulin formulation is safe and did not elicit any adverse events or discomfort to the healthy volunteers. A Phase II, trial is planned to start in 2014. Clearly more opportunities exist to expand the technology to other actives. Typically, films are produced either by film casting or heat extrusion. The polymers used to form the films are selected depending on the film thickness required as well as compatibility with the drug. A detailed review by Dixit and Puthli (2009) addresses materials used in TFT, critical manufacturing aspects and applications.

Iontophoresis has been investigated by a number of researchers with promising results reported recently for galantamine in pigs (Giannola et al., 2010) and for naltrexone in man (Paderni et al., 2013). These short-term studies describe an "Intellidrug®" device which consists of intraoral and extraoral sections. The intraoral part consists of an outlet system embedded in a silicone-made mouth prop, whereas the extra-oral part contains a drug reservoir, a syringe pump, a flow sensor and a power source for the flow sensor. No irritation or histological damage was reported for the studies in man (conducted over 9 days) with further studies currently planned to test long-term use and wearability of the device.

Generex announced the completion of Phase III trials on a spray formulation of recombinant human insulin (Oral-Lyn®) for buccal administration in 2013. A metered dose type device is used to deliver the equivalent of one unit of insulin per spray to the oral cavity. The actual formulation is based on patented technology (RapidMist®) where the active is in solution with a combination of absorption enhancers and other excipients classified generally recognized as safe. Oral-Lyn™ significantly lowered the HbA1c at 6 weeks and 12 weeks compared to baseline ($p < 0.05$) while injected human regular insulin did not significantly lower the HbA1c until 12 weeks. The formulation also resulted in a significantly lower HbA1c at 6 weeks than did injected regular insulin ($p < 0.05$). At 12 weeks the HbA1c for both groups were statistically comparable (www.generex.com).

6. Conclusions

OTDD continues to attract the attention of academic and industrial scientists even though few new formulations have been brought to market in recent years. One of the problems appears to be the more limited characterisation of the permeation pathways in the oral cavity compared with skin and nasal routes of delivery. Recent advances in our understanding of the extent to which ionized molecules permeate through buccal epithelium are encouraging as are the emergence of new analytical techniques to study the oral cavity. Development of in silico models predictive of buccal and sublingual permeation has also been progressed.

The features of the oral cavity are an inherent challenge to effective OTDD, specifically the limited surface area of this region as well as its salivary content. The number of actives which has been studied for delivery via this route using in vitro models is impressive but the doses employed in a number of these studies are not representative of typical clinical doses. Tissue integrity in in vitro models is limited and drug metabolism has not been explored in any detail to date. Moreover, the environment of the oral cavity cannot be simulated effectively using such in vitro models.

Regulatory requirements for OTDD are also likely to be a significant burden for pharmaceutical companies. In contrast to transdermal delivery, effective correlations between in vitro permeation testing and in vivo performance have yet to be demonstrated for OTDD. Currently the US FDA is working towards a method to validate the safety and effectives of medicated chewing gums but specific guidelines for OTDD have not yet been developed. There does not appear to be instances in which

specific drugs have been designed for buccal delivery. Given the advantages of this route perhaps this could be a prospect for the future. However, more predictive algorithms would be required to fulfil this proposition. These can only be developed when a mechanistic knowledge of the routes of penetration has been established.

Acknowledgement

We thank Dr. Ossama M. Sayed for provision of experimental data.

References

Adeleke, O.A., Pillay, V., du Toit, Y.E., 2010. Construction and in vitro characterization of an optimized porosity-enabled amalgamated matrix for sustained transbuccal drug delivery. Int. J. Pharm. 391, 79–89.
Adrian, C.L., Olin, H.B., Dalhoff, K., Jacobsen, J., 2006. In vivo human buccal permeability of nicotine. Int. J. Pharm. 06, 196–202.
Amores, S., Lauroba, J., Calpena, A., Colom, H., Gimeno, A., Domenech, J., 2014. A comparative ex vivo drug permeation study of beta-blockers through porcine buccal mucosa. Int. J. Pharm. 468, 50–54.
Artusi, M., Santi, P., Colombo, P., Junginger, H.E., 2003. Buccal delivery of thiocolchicoside: in vitro and in vivo permeation studies. Int. J. Pharm. 250, 203–213.
Avachat, A.M., Gujar, K.N., Wagh, K.V., 2013. Development and evaluation of tamarind seed xyloglucan-based mucoadhesive buccal films of rizatriptan benzoate. Carbohydr. Polym. 91, 537–542.
Beckett, A.H., Triggs, E.J., 1967. Buccal absorption of basic drugs and its application as an in vivo model of passive drug transfer through lipid membranes. J. Pharm. Pharmacol. 19, 31S–41S.
Beckett, A.H., Moffat, A.C., 1968. The influence of alkyl substitution in acids on their performance in the buccal absorption test. J. Pharm. Pharmacol. 20, 239S–247S.
Beckett, A.H., Moffat, A.C., 1969a. The influence of substitution in phenylacetic acids on their performance in the buccal absorption test. J. Pharm. Pharmacol. 21, 139S–143S.
Beckett, A.H., Moffat, A.C., 1969b. Correlation of partition coefficients in Il-heptane-aqueous systems with buccal absorption data for a series of amines and acids. J. Pharm. Pharmacol. 21, 144S–150S.
Beckett, A.H., Moffat, A.C., 1970. Kinetics of buccal absorption of some carboxylic acids and the correlation of the rate constants and n-heptane: aqueous phase partition coefficients. J. Pharm. Pharmacol. 22, 15–19.
Beckett, A.H., Moffat, A.C., 1971. The buccal absorption of some barbiturates. J. Pharm. Pharmacol. 23, 15–18.
Beckett, A.H., Pickup, M.E., 1975. A model for steroid transport across biological membranes. J. Pharm. Pharmacol. 27, 226–234.
Bird, A.P., Faltinek, J.R., Shojaei, A.H., 2001. Transbuccal peptide delivery: stability and in vitro permeation studies on endomorphin-1. J. Control. Release 73, 31–36.
Birudaraj, R., Berner, B., Shen, S., Li, X., 2005. Buccal permeation of buspirone: mechanistic studies on transport pathways. J. Pharm. Sci. 94, 70–78.
Campisi, G., Giannola, L.I., Florena, A.M., De Caro, V., Schumacher, A., Gottsche, T., Paderni, C., Wolff, A., 2010. Bioavailability in vivo of naltrexone following transbuccal administration by an electronically-controlled intraoral device: a trial on pigs. J. Control. Release 145, 214–220.
Caon, T., Pan, Y., Simoes, C.M., Nicolazzo, J.A., 2014. Exploiting the buccal mucosa as an alternative route for the delivery of donepezil hydrochloride. J. Pharm. Sci. 103, 1643–1651.
Cappello, B., De Rosa, G., Giannini, L., La Rotonda, M.I., Mensitieri, G., Miro, A., Quaglia, F., Russo, R., 2006. Cyclodextrin-containing poly(ethyleneoxide) tablets for the delivery of poorly soluble drugs: potential as buccal delivery system. Int. J. Pharm. 319, 63–70.
Charde, S., Mudgal, M., Kumar, L., Saha, R., 2008. Development and evaluation of buccoadhesive controlled release tablets of lercanidipine. AAPS PharmSciTech 9, 182–190.
Cid, Y.P., Pedrazzi, V., de Sousa, V.P., Pierre, M.B., 2012. In vitro characterization of chitosan gels for buccal delivery of celecoxib: influence of a penetration enhancer. AAPS PharmSciTech. 13, 101–111.
Claus, R., Haussler, S., Lacorn, M., 2007. Rise of testosterone, nortestosterone, and 17beta-estradiol concentrations in peripheral blood plasma of pigs after sublingual application in vivo. Food Chem. Toxicol. 45, 225–228.
Collins, P., Laffoon, J., Squier, C.A., 1981. Comparative structure of porcine oral epithelia. IADR Progr. Abst. 60, 933.
Das, N., Madan, P., Lin, S., 2012. Statistical optimization of insulin-loaded Pluronic F-127 gels for buccal delivery of basal insulin. Pharm. Dev. Technol. 17, 363–374.
Dawson, D.V., Drake, D.R., Hill, J.R., Brogden, K.A., Fischer, C.L., Wertz, P.W., 2013. Organization, barrier function and antimicrobial lipids of the oral mucosa. Int. J. Cosmet. Sci. 35, 220–223.
De Caro, V., Giandalia, G., Siragusa, M.G., Paderni, C., Campisi, G., Giannola, L.I., 2008. Evaluation of galantaminetransbuccal absorption by reconstituted human oral epithelium andporcine tissue as buccal mucosa models: part I. Eur. J. Pharm. Biopharm. 70, 869–873.
De Caro, V., Giandalia, G., Siragua, M.G., Sutera, F.M., Giannola, L.I., 2012. New prospective in treatment of Parkinson's disease: studies on permeation of ropinirolethroughbuccal mucosa. Int. J. Pharm. 429, 78–83.
Deneer, V.H.M., Drese, G.B., Roemele, P.E.H., Verhoef, J.C., Lie-A-Huen, L., Kingma, J.H., Brouwers, J.R.B.J., Junginger, H.E., 2002. Buccal transport of flecainideandsotalol: effect of a bile salt and ionization state. Int. J. Pharm. 241, 127–134.
Diaz Del Consuelo, I., Falson, F., Guy, R.H., Jacques, Y., 2005. Transport of fentanyl through pig buccal and esophageal epithelia in vitro: influence of concentration and vehicle pH. Pharm. Res. 22, 1525–1529.
Dixit, R.P., Puthli, S.P., 2009. Oral strip technology: overview and future potential. J. Control. Release 139, 94–107.
El-Samaligy, M.S., Yahia, S.A., Basalious, E.B., 2004. Formulation and evaluation of diclofenac sodium buccoadhesive discs. Int. J. Pharm. 286, 27–39.
Figueiras, A., Hornbach, J., Veiga, F., Bernkop-Schnürch, A., 2009. In vitro evaluation of natural and methylated cyclodextrins as buccal permeation enhancing system for omeprazole delivery. Eur. J. Pharm. Biopharm. 71, 339–345.
Gandhi, R.B., Robinson, J.R., 1994. Oral cavity as a site for bioadhesive drug delivery. Adv. Drug Deliv. Rev. 13, 43–74.
Giannola, L.I., De Caro, V., Giandalia, G., Siragusa, M.G., D'Angelo, M., Lo Muzio, L., Campisi, G., 2005. Transbuccal tablets of carbamazepine: formulation, release and absorption pattern. Int. J. Immunopathol. Pharmacol. 18, 21–31.
Giannola, L.I., De Caro, V., Giandalia, G., Siragusa, M.G., Tripodo, C., Florena, A.M., Campisi, G., 2007. Release of naltrexone on buccal mucosa: permeation studies, histological aspects and matrix system design. Eur. J. Pharm. Biopharm. 67, 425–433.
Giannola, L.I., Paderni, C., De Caro, V., Florena, A.M., Wolff, A., Campisi, G., 2010. New prospectives in the delivery ofgalantamine for elderly patients using the IntelliDrug intraoral device: in vivo animal studies. Curr. Pharm. Design 16, 653–659.
Gilles, P., Ghazali, F.A., 1996. Systemic oral mucosal drug delivery systems and delivery systems. In: Rathbone, M.J. (Ed.), Oral Mucosal Drug Delivery. Marcel Dekker Inc., New York, pp. 241–285.
Gore, A.V., Liang, A.C., Chien, Y.W., 1998. Comparative biomembrane permeation of tacrine using Yucatan minipigs and domestic pigs as the animal model. J. Pharm. Sci. 87, 441–447.
Goswami, T., Jasti, B.R., Li, X., 2009. Estimation of the theoretical pore sizes of the porcine oral mucosa for permeation of hydrophilic permeants. Arch. Oral Biol. 54, 577–578.
Goswami, T., Kokate, A., Jasti, B.R., Li, X., 2013. In silico model of drug permeability across sublingual mucosa. Arch. Oral Biol. 58, 545–551.
Harris, D., Robinson, J.R., 1992. Drug delivery via the mucous membranes of the oral cavity. J. Pharm. Sci. 81, 1–10.
Heaney, T.G., Jones, R.S., 1978. Histological investigation of the influence of adult porcine alveolar mucosal connective tissue on epithelial differentiation. Arch. Oral Biol. 23, 713–717.
Heemstra, L.B., Finnin, B.C., Nicolazzo, J.A., 2010. The buccal mucosa as an alternative route for the systemic delivery of risperidone. J. Pharm. Sci. 99, 4584–4592.
Herrera, J.L., Lyons 2nd, M.F., Johnson, L.F., 1988. Saliva: its role in health and disease. J. Clin. Gastroenterol. 10, 569–578.
Holm, R., Meng-Lund, E., Andersen, M.B., Jespersen, M.L., Karlsson, J.J., Garmer, M., Jørgensen, E.B., Jacobsen, J., 2013. In vitro, ex vivo and in vivo examination of buccal absorption of metoprolol with varying pH inTR146 cell culture, porcine buccal mucosa and Gøttingen minipigs. Eur. J. Pharm. Sci. 49, 117–124.
Hoogstraate, C., Nagelkerke, J.F., Senel, S., Verhoef, J.C., Junginger, H.E., Bodde, H.E., 1994. Diffusion rates and transport pathways offluorescein isothiocyanate (FITC)-labeled model compounds through buccal epithelium. Pharm. Res. 11, 83–89.
Hoogstraate, A.J., Verhoef, J.C., Pijpers, A., van Leengoed, L.A., Verheijden, J.H., Junginger, H.E., Bodde, H.E., 1996. In vivo buccal delivery of the peptide drug buserelin with glycodeoxycholate as an absorption enhancer in pigs. Pharm. Res. 13, 1233–1237.
Hu, L., Silva, S.M., Damaj, B.B., Martin, R., Michniak-Kohn, B.B., 2011. Transdermal and transbuccal drug delivery systems: enhancement using iontophoretic and chemical approaches. Int. J. Pharm. 421, 53–62.
Jacobsen, J., 2001. Buccal iontophoretic delivery of atenolol. HCl employing a new in vitro three-chamber permeation cell. J. Control. Release 70, 83–95.
Jacobsen, J., Nielsen, E.B., Brondum-Nielsen, K., Christensen, M.E., Olin, H.B., Tommerup, N., Rassing, M.R., 1999. Filter-grown TR146 cells as an in vitro model of human buccal epithelial permeability. Eur. J. Oral Sci. 107, 138–146.
Jain, S.K., Jain, A., Gupta, Y., Kharya, A., 2008. Design and development of a mucoadhesive buccal film bearing progesterone. Pharmazie 63, 129–135.
Kamel, R., Mahmoud, A., El-Feky, G., 2012. Double-phase hydrogel for buccal delivery of tramadol. Drug Dev. Ind. Pharm. 38, 468–483.
Kokate, A., Li, X., Singh, P., Jasti, B.R., 2008a. Effect of thermodynamic activities of the unionized and ionized species on drug flux across buccal mucosa. J. Pharm. Sci. 97, 4294–4306.
Kokate, A., Li, X., Jasti, B., 2008b. Effect of drug lipophilicity and ionization on permeability across the buccal mucosa: a technical note. AAPS PharmSciTech 9, 501–504.
Kokate, A., Li, X., Williams, P.J., Singh, P., Jasti, B.R., 2009. In silico prediction of drug permeability across buccal mucosa. Pharm. Res. 26, 1130–1139.
Kulkarni, U., Mahalinghan, R., Pather, S.I., Jasti, B., 2009. Porcine buccal mucosa as an in vitro model: relative contribution of epithelium and connective tissue as permeability barriers. J. Pharm. Sci. 98, 471–483.

Kulkarni, U., Mahalingam, R., Pather, I., Li, X., Jasti, B., 2010. Porcine buccal mucosa as in vitro model: effect of biological and experimental variables. J. Pharm. Sci. 99, 1265–1277.
Kulkarni, U.D., Mahalingam, R., Li, X.X., Pather, I., Jasti, B., 2011. Effect of experimental temperature on the permeation of model diffusants across porcine buccalmucosa. AAPS PharmSciTech 12, 579–586.
Kurosaki, Y., Nishimura, H., Terao, K., Nakayama, T., Kimura, T., 1992. Existence of a specialized absorption mechanism for cefadroxil, an aminocephalosporin antibiotic, in the human oral cavity. Int. J. Pharm. 82, 165–169.
Kurosaki, Y., Yano, K., Kimura, T., 1998. Perfusion cells for studying regional variation in oral mucosal permeability in humans. 2. A specialized transport mechanism in D-glucose absorption exists in dorsum of tongue. J. Pharm. Sci. 87, 613–615.
Langoth, N., Kalbe, J., Bernkop-Schnürch, A., 2005. Development of a mucoadhesive and permeation enhancing buccal delivery system for PACAP (pituitary adenylate cyclase-activating polypeptide). Int. J. Pharm. 296, 103–111.
Lee, J., Kellaway, I.W., 2000. Combined effect of oleic acid and polyethylene glycol 200 on buccal permeation of [D-ala2, D-leu5]enkephalin from a cubic phase of glyceryl monooleate. Int. J. Pharm. 204, 137–144.
Lee, J., Choi, Y.W., 2003. Enhanced ex vivo buccal transport of propranolol: evaluation of phospholipids as permeation enhancers. Arch. Pharm. Res. 26, 421–425.
Lesch, C.A., Squier, C.A., Cruchley, A., Williams, D.M., Speight, P., 1989. The permeability of human oral mucosa and skin to water. J. Dent. Res. 68, 1345–1349.
Maffei, P., Lombardi Borgia, S., Sforzini, A., Bergamante, V., Ceschel, G.C., Fini, A., Ronchi, C., 2004. Mucoadhesive tablets for buccal administration containing sodium nimesulide. Drug Deliv. 11, 225–230.
Mahalingam, R., Ravivarapu, H., Redkar, S., Li, X., Jasti, B.R., 2007. Transbuccal delivery of 5-aza-2 -deoxycytidine: effects of drug concentration, buffer solution, and bile salts on permeation. AAPS PharmSciTech 13, E55.
Mashru, R.C., Sutariva, V.B., Sankalia, M.G., Sankalia, J.M., 2005a. Effect of pH on in vitro permeation of ondansetron hydrochloride across porcine buccal mucosa. Pharm. Dev. Technol. 10, 241–247.
Mashru, R., Sutariya, V., Sankalia, M., Sankalia, J., 2005b. Transbuccal delivery of lamotrigine across porcine buccal mucosa: in vitro determination of routes of buccal transport. J. Pharm. Pharm. Sci. 8, 54–62.
Meng-Lund, E., Jacobsen, J., Jin, L., Janfelt, C., Holm, R., Mullertz, A., Nicolazzo, J.A., 2014. Azone® decreases the buccal mucosal permeation of diazepam in a concentration-dependent manner via a reservoir effect. J. Pharm. Sci. 103, 1133–1141.
Miro, A., Rondinone, A., Nappi, A., Ungaro, F., Quaglia, F., La Rotonda, M.I., 2009. Modulation of release rate and barrier transport of Diclofenac incorporated in hydrophilic matrices: role of cyclodextrins and implications in oral drug delivery. Eur. J. Pharm. Biopharm. 72, 76–82.
Murrell, W.H., 1882. Nitroglycerin in Angina Pectoris. HK Lewis, London, pp. 1–70.
Nair, M.K., Chetty, D.J., Ho, H., Chien, Y.W., 1997. Biomembrane permeation of nicotine: mechanistic studies with porcine mucosae and skin. J. Pharm. Sci. 86, 257–262.
Nicolazzo, J.A., Reed, B.L., Finnin, B.C., 2003. The effect of various in vitro conditions on the permeability characteristics of the buccal mucosa. J. Pharm. Sci. 92, 2399–2410.
Nicolazzo, J.A., Reed, B.L., Finnin, B.C., 2004. Modification of buccal drug delivery following pretreatment with skin penetration enhancers. J. Pharm. Sci. 93, 2054–2063.
Nicolazzo, J.A., Reed, B.L., Finnin, B.C., 2005. Enhanced buccal mucosal retention and reduced buccal permeability of estradiol in the presence of padimate O and Azone: a mechanistic study. J. Pharm. Sci. 94, 873–882.
Nielsen, H.M., Rassing, M.R., 2000. TR146 cells grown on filters as a model of human buccal epithelium: IV. Permeability of water, mannitol, testosterone and beta-adrenoceptor antagonists. Comparison to human, monkey and porcine buccal mucosa. Int. J. Pharm. 194, 155–167.
Nielsen, H.M., Verhoef, J.C., Ponec, M., Rassing, M.R., 1999. TR146 cells grown on filters as a model of human buccal epithelium: permeability of fluorescein isothiocyanate-labelled dextrans in the presence of sodium glycocholate. J. Control. Release 60, 223–233.
Nielsen, H.M., Rassing, M.R., 2002. Nicotine permeability across the buccal TR146 cell culture model and porcine buccal mucosa in vitro: effect of pH and concentration. Eur. J. Pharm. Sci. 16, 151–157.
Oh, D.H., Chun, K.H., Jeon, S.O., Kang, J.W., Lee, S., 2011. Enhanced transbuccal salmon calcitonin (sCT) delivery: effect of chemical enhancers and electrical assistance on in vitro sCT buccal permeation. Eur. J. Pharm. Biopharm. 79, 357–363.
Ojewole, E., Mackraj, I., Akhundov, K., Hamman, J., Viljoen, A., Olivier, E., Wesley-Smith, J., Govender, T., 2012. Investigating the effect of Aloe vera gel on the buccal permeability of didanosine. Planta Med. 78, 354–361.
Paderni, C., Campisi, G., Schumacher, A., Gottsche, T., Giannola, L.I., De Caro, V., Wolff, A., 2013. Controlled delivery of naltrexone by an intraoral device: in vivo study on human subjects. Int. J. Pharm. 452, 128–134.
Palem, C.R., Gannu, R., Yamsani, S.K., Yamsani, V.V., Yamsani, M.R., 2011a. Development of bioadhesive buccal tablets for felodipine and pioglitazone in combined dosage form: in vitro, ex vivo, and in vivo characterization. Drug Deliv. 18, 344–352.
Palem, C.R., Gannu, R., Doodipala, N., Yamsani, V.V., Yamsani, M.R., 2011b. Transmucosal delivery of domperidone from bilayered buccal patches: in vitro, ex vivo and in vivo characterization. Arch. Pharm. Res. 34, 1701–1710.
Pimlott, S.J., Addy, M., 1985. A study into the mucosal absorption of isosorbide dinitrate at different intraoral sites. Oral Surg. Oral Med. Oral Pathol. 59, 145–148.
Prasanna, R.I., Anitha, P., Chetty, C.M., 2011. Formulation and evaluation of bucco-adhesive tablets of sumatriptan succinate. Int. J. Pharm. Investig. 1, 182–191.
Pudney, P.D., Bonnist, E.Y., Caspers, P.J., Gorce, J.P., Marriot, C., Puppels, G.J., Singleton, S., van der Wolf, M.J., 2012. A new in vivo Raman probe for enhanced applicability to the body. Appl. Spectrosc. 66, 882–891.
Puratchikody, A., Prasanth, V.V., Mathew, S.T., Kumar, B.A., 2011. Development and characterization of mucoadhesive patches of salbutamol sulfate for unidirectionalbuccal drug delivery. Acta Pharm. 61, 157–170.
Rambharose, S., Ojewole, E., Mackraj, I., Govender, T., 2014a. Comparative buccal permeability enhancement of didanosine and tenofovir by potential multifunctional polymeric excipients and their effects on porcine buccal histology. Pharm. Dev. Technol. 19, 82–90.
Rambharose, S., Ojewole, E., Branham, M., Kalhapure, R., Govender, T., 2014b. High-energy ball milling of saquinavir increases permeability across the buccal mucosa. Drug Dev. Ind. Pharm. 40, 639–648.
Rao, S., Song, Y., Peddie, F., Evans, A.M., 2011. Particle size reduction to the nanometer range: a promising approach to improve buccal absorption of poorly water-soluble drugs. Int. J. Nanomedicine 6, 1245–1251.
Rathbone, M.J., 1991. Human buccal absorption. I. A method for estimating the transfer kinetics of drugs across the human buccal membrane. Int. J. Pharm. 69, 103–108.
Rupniak, H.T., Rowlatt, C., Lane, E.B., Steele, J.G., Trejdosiewicz, L.K., Laskiewicz, B., Povey, S., Hill, B.T., 1985. Characteristics of four new human cell lines derived from squamous cell carcinomas of the head and neck. J. Natl. Cancer Inst. 75, 621–635.
Sekhar, K.C., Naidu, K.V., Vishnu, Y.V., Gannu, R., Kishan, V., Rao, Y.M., 2008. Transbuccal delivery of chlorpheniramine maleate from mucoadhesive buccal patches. Drug Deliv. 15, 185–191.
Senel, S., Duchêne, D., Hincal, A.A., Capan, Y., Ponchel, G., 1998. In vitro studies on enhancing effect of sodium glycocholate on transbuccal permeation of morphine hydrochloride. J. Control. Release 51, 107–113.
Senel, S., Kremer, M.J., Kas, S., Wertz, P.W., Hincal, A.A., Squier, C.A., 2000. Enhancing effect of chitosan on peptide drug delivery across buccal mucosa. Biomaterials 21, 2067–2071.
Shidhaye, S.S., Thakkar, P.V., Dand, N.M., Kadam, V.J., 2010. Buccal drug delivery of pravastatin sodium. AAPS PharmSciTech 11, 416–424.
Shojaei, A.H., Berner, B., Xiaoling, L., 1998. Transbuccal delivery of acyclovir: I. In vitro determination of routes of buccal transport. Pharm. Res. 15, 1182–1188.
Shojaei, A.H., Khan, M., Lim, G., Khosravan, R., 1999. Transbuccal permeation of a nucleoside analog, dideoxycytidine: effects of menthol as a permeation enhancer. Int. J. Pharm. 192, 139–146.
Slomiany, B.L., Piotrowski, J., Majka, J., Liau, Y.H., Slomiany, A., 1993. Identification of buccal mucosal mucin receptor. Biochem. Mol. Biol. Int. 31, 1091–1099.
Slomiany, B.L., Murty, V.L., Piotrowski, J., Slomiany, A., 1996. Salivary mucins in oral mucosal defense. Gen. Pharmacol. 27, 761–771.
Squier, C.A., Rooney, L., 1976. The permeability of keratinized and nonkeratinized oral epithelium to lanthanum in vivo. J. Ultrastruct. Res. 54, 286–295.
Squier, C.A., Hall, B.K., 1985. In-vitro permeability of porcine oral mucosa after epithelial separation, stripping and hydration. Arch. Oral Biol. 30, 485–491.
Squier, C.A., 1991. The permeability of oral mucosa. Crit. Rev. Oral Biol. Med. 2, 13–32.
Squier, C.A., Johnson, N.W., Hopps, R.M., 1976. Regional differences of the oral mucosa. Human Oral Mucosa Developrnent, Structure and Function. Blackwell, Oxford, pp. 73–86.
Squier, C.A., Wertz, P.W., 1996. Structure and function of the oral mucosa and implications for drug delivery. In: Rathbone, M.J. (Ed.), Oral Mucosal Drug Delivery. Marcel Dekker Inc., New York, pp. 1–26.
Squier, C., Brogden, K., 2011. Human Oral Mucosa: Development, Structure and Function, 1st ed. Wiley-Blackwell, UK, pp. 77–97.
Tabak, L.A., Levine, M.J., Mandel, I.D., Ellison, S.A., 1982. Role of salivary mucins in the protection of the oral cavity. J. Oral Pathol. 11, 1–17.
Tucker, I.G., 1988. A method to study the kinetics of oral mucosal drug absorption from solutions. J. Pharm. Pharmacol. 40, 679–683.
van der Bijl, P., Penkler, L., van Eyk, A.D., 2000. Permeation of sumatriptan through human vaginal and buccal mucosa. Headache 40, 137–141.
Veuillez, F., Kalia, Y.N., Jacques, Y., Deshusses, J., Buri, P., 2001. Factors and strategies for improving buccal absorption of peptides. Eur. J. Pharm. Biopharm. 51, 93–109.
Wang, Y., Zuo, Z., Lee, K.K., Chow, M.S., 2007. Evaluation of HO-1-u-1 cell line as an in vitro model for sublingual drug delivery involving passive diffusion – initial validation studies. Int. J. Pharm. 334, 27–34.
Wang, Y., Zuo, Z., Chow, M.S., 2009. HO-1-u-1 model for screening sublingual drug delivery – influence of pH, osmolarity and permeation enhancer. Int. J. Pharm. 370, 68–74.
Young, B., Lowe, J.S., Stevens, A., Heath, J.W., 2006. Wheater's Functional Histology, 5th ed. Churchill Livingstone – Elsevier, UK, pp. 82–101.
Yuan, Q., Fu, Y., Kao, W.J., Janigro, D., Yang, H., 2011. Transbuccal delivery of CNS therapeutic nanoparticles: synthesis, characterization, and in vitro permeation studies. ACS Chem. Neurosci. 2, 676–683.
Zhang, H., Robinson, J.R., 1996. Routes of drug transport across oral mucosa. In: Rathbone, M.J. (Ed.), Oral Mucosal Drug Delivery. Marcel Dekker Inc., New York, pp. 51–63.

Pharmaceutical Development and Technology, 2011; 00(00): 000–000

ISSN 1083-7450 print/ISSN 1097-9867 online
DOI: 10.3109/10837450.2011.646425

informa
healthcare

RESEARCH ARTICLE

Preparation and characterization of mosapride citrate inclusion complexes with natural and synthetic cyclodextrins

Adel A. Ali and Ossama M. Sayed

Department of Pharmaceutics and industrial pharmacy, Faculty of Pharmacy, Beni Suef University, Beni Suef, Egypt

Abstract

The aim of this work was to investigate the inclusion complexes between mosapride citrate and SBE$_7$$\beta$-CD in comparison with the natural β-CD to enhance its bioavailability by improving the solubility and dissolution rate. The complexation efficiency value of SBE$_7$$\beta$-CD was higher than that for β-CD. Solid binary systems of mosapride citrate with CDs were prepared by physical mixing, kneading and freeze-drying techniques at molar ratio of 1:1(drug:CD). Physicochemical characterization of the prepared systems was studied using X-ray diffractometry, differential scanning calorimetry, Fourier-transform infrared spectroscopy and scanning electron microscopy (SEM). Amorphous drug was detectable to large extent in inclusion complexes prepared using the freeze-drying technique. From the dissolution study of different inclusion complexes in simulated saliva solution (pH 6.8), we could concluded that irrespective of the preparation technique, the systems prepared using SBE$_7$$\beta$-CD showed better performance than the corresponding ones prepared using β-CD. In addition, the freeze-drying technique showed superior dissolution enhancement than other methods especially when combined with the SBE$_7$$\beta$-CD

Keywords: Mosapride citrate, cyclodextrins, inclusion complexes, physicochemical characterization, *in vitro* dissolution

Introduction

Mosapride citrate is a novel gastrointestinal prokinetic agent which is used in different gastrointestinal complaints as poor appetite, vomiting associated with chronic gastritis and reflux esophagitis.[1]

It facilitates acetylcholine release from the enteric cholinergic neurons, and in contrast to cisapride, it does not block K^+ channels or D_2 dopaminergic receptors and selectively acts on serotonin (5-HT_4) receptors.[2–4]

Mosapride citrate is a benzamide agent (Figure 1) whose structure contains a morpholine ring[5,6] The poor solubility and wettability of this drug give rise to difficulties in pharmaceutical formulation meant for oral use, which may lead to variation in its bioavailability.

Inclusion of drugs into cyclodextrins (CDs) have been introduced many advantages reported in scientific literatures such as increased solubility, enhanced bioavailability, improved stability, masking of bad test or odor, reduced volatility, transformation of liquid or gas into solid form, reduced side effect, and the possibility of a drug release system, and so on.[7–14]

Only the natural CDs were used, but due to the poor aqueous solubility, derivatives of these CDs, with increased aqueous solubility properties, have been developed.[15]

Sulfobutyl Ether$_7$ β-cyclodextrin (Captisol®) is a polyanionic CD derivative, with greater solubility in water than the parent CD.[16] The inclusion ability of SBE$_7$$\beta$-CD is generally higher than that of β-CD due to the hydrophobic butyl side arms that extend the hydrophobic cavity of the CD.[17]

The work in this study is an attempt to improve the solubility and dissolution rate of mosapride citrate via inclusion complexes with β-CD and SBE$_7$$\beta$-CD to be formulated into buccal drug delivery systems (gels or films), thereby increasing its bioavailability and therapeutics efficiency.

Different techniques were as physical mixing, kneading and freeze drying are used to prepare the drug CD

Address for Correspondence: Department of Pharmaceutics and industrial pharmacy, Faculty of Pharmacy, Beni Suef University, Beni Suef, Egypt. Phone: +2 082 2317958, +2 010 3897691. E-mail: dr_adelahmedali@yahoo.com

(Received 25 September 2011; revised 27 November 2011; accepted 30 November 2011)

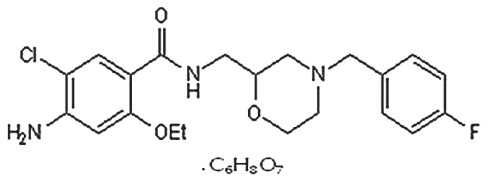

Figure 1. Chemical structure of mosapride citrate.

inclusion complexes were at 1:1(drug to CD) molar ratio.

The physicochemical characterization of drug CD inclusion complexes were performed using X-ray diffractometry (XRD), differential scanning calorimetry (DSC), Fourier-transform infrared (FTIR), scanning electron microscopy (SEM) and *in vitro* dissolution study.

Materials and methods

Materials

Mosapride citrate was obtained as a gift sample from Marcyrl pharma (Egypt), β-cyclodextrin (Kleptose®) was obtained as a gift sample from Roquette (France), Sulfobutyl Ether$_7$ β-cyclodextrin (Captisol®) was obtained as a gift sample from Cydex pharmaceuticals (USA), all other ingredients and solvents used were of analytical grade.

Phase solubility studies

According to the phase solubility technique established by Higuchi and Connors[18], the effects of CDs on the solubility of mosapride citrate were investigated.

Mosapride citrate in an excess amounts were added to 50 mL simulated saliva solutions (pH 6.8) containing increasing concentrations of the CDs (0.002–0.01 mole/L based on the maximum solubility of β-CD in water at 37°C).

The obtained suspensions were shaken at 37°C for 72 h in a thermostatically controlled shaking water bath (Memmert, France). After equilibrium, aliquots were withdrawn, filtered through a membrane filter 0.45 um (Sartorious, AG Germany), and the drug concentration was determined by reverse phase HPLC at the following conditions:

The HPLC system (HP Agilent 1100 HPLC System, USA) consisted of a binary pump (HP G1312A Binary Pump, USA), and a UV-vis detector (HP G1314A Variable Wavelength Detector, USA) and Column (Supelco column LC-18, 5 µm, 150 mm × 4.6 mm).

The mobile phase was methanol: 20 mM KH_2PO_4 (70:30% v/v) containing 10 mM triethylamine and pH adjusted at 7, with a flow rate of 1mL/min. The detection wavelength was set at 274 nm and the retention time was 5.4 min. All the data were the average of three determinations.

Phase solubility diagrams were obtained by plotting the solubility of mosapride citrate (mole/L), versus the concentrations of the CDs used (mole/L).

The complexation efficiency (CE), as a parameter indicating the solubilizing power of the CDs towards the drug, was calculated from the straight line of the phase solubility diagrams according to the equation:

$$CE = S_o.K_{1:1} = \text{slope} / (1 - \text{slope})$$

Where S_o represents the drug solubility in the absence of CDs, $K_{1:1}$ is the apparent stability constant, where $K_{1:1} = \text{slope}/S_o\,(1 - \text{slope})$.[19]

Preparation of drug-CDs inclusion complexes

Based on 1:1 molar ratio, different inclusion complexes of mosapride citrate and CDs were prepared by the following methods:

Physical mixing method

In a porcelain mortar, the calculated amounts of mosapride citrate and CDs that had previously been sieved through sieve no 60, were mixed for 30 min.

Kneading method

The calculated a mounts of each CD were dissolved in a small amount of water to form a paste.

The drug component dissolved in a small amount of methanol has been added to the paste portionwise with trituration for several hours.

After complete evaporation of the solvents, the remaining mass was dried in a desiccator at room temperature for 72 h, then pulverized and passed through sieve no 60.

Freeze-drying method

Appropriate quantities of mosapride citrate and CDs were dissolved in a mixture of distilled water and methanol (50:50 % v/v). The clear solutions were frozen, and subsequently freeze dried for 48 h at –50°C using a freeze dryer (Snijders Scientific B.V, Netherlands). The obtained mass was pulverized and passed through sieve no 60.

Physicochemical characterization of mosapride citrate-CDs inclusion complexes

X-ray diffractograms, DSC thermograms and FTIR spectra were recorded for pure mosapride citrate, pure CDs, and their inclusion complexes prepared by different techniques.

X-ray diffractometry

The X-ray diffraction patterns were recorded at room temperature using a Scintag diffractometer (XGEN-4000, Scintag Corp, USA). The samples were irradiated with Ni-filtered Cu K_α radiation and the work conditions were 45 kV voltage, 40 mA current and scanning rate of 1.2°/min over a diffraction angle of 2θ and range of 4°–50°.

Differential scanning calorimetry

Five milligrams samples were placed into pierced aluminum container and analyzed by DS Calorimeter (DSC-50 Schimadzu, Japan). The studies were performed under

nitrogen gas atmosphere in the temperature range of 20°C to 250°C at a heating rate of 5°C/min. The peak temperatures were determined after calibration with standard (purified indium 99.9%).

Fourier-transform infrared spectroscopy

Fourier-transform infrared spectra were recorded on IR spectrophotometer (Shimadzu IR–435, Kyoto, Japan). Samples weighing about 2 to 3 mg were mixed with about 400 mg of dry KBr and compressed into discs. The IR spectra were recorded at scanning range from 400–4000 cm^{-1} and resolution of 4 cm^{-1}.

Scanning electron microscopy

The powdered samples were sprinkled onto double-sided carbon tape fixed on aluminum stubs and coated with a thin gold layer by sputter coater unit (SPI, sputter, USA). The aluminum stubs were placed in the vacuum chamber of a scanning electron microscope (Joel, JSM-6510LA, Japan). Surface morphology identification of the powder of different samples was done at magnifications of 250×, 1000× or 1500× and an accelerating voltage of 30 kV.

Determination of solubility of mosapride citrate-CDs inclusion complexes

To determine the solubility of the prepared inclusion complexes in phosphate buffer (pH 6.8), an excess amount of each inclusion complex was added to 5 mL of the phosphate buffer solution in test tubes sealed with stoppers.

The test tubes were vortex mixed for 2 min and then kept in a constant temperature shaking bath maintained at 37 ± 0.5°C for 72 h. A portion of solution was withdrawn and then filtered through 0.45 um membrane filter (Sartorious, AG Germany) and adequately diluted with phosphate buffer solution.

As a control experiment, the solubility of pure mosapride citrate was determined in a similar manner.

The drug concentration was determined by reverse phase HPLC as mentioned in phase solubility studies section.

In vitro dissolution studies

The dissolution of pure mosapride citrate and the prepared inclusion complexes were tested in 900 mL of simulated saliva solutions (pH 6.8) using a USP dissolution tester, apparatus II (Hanson Research, SR 8 plus model, Chatsworth, USA). A sample equivalent to 5 mg mosapride citrate of the prepared systems (from the powder fraction passed through sieve No.60 and retained on sieve No.80) was sprinkled on the surface of the dissolution medium. The stirring speed was 100 rpm and the temperature was maintained at 37 ± 0.5°C.

Aliquots each of 5 mL was withdrawn from the dissolution medium through a 0.45 um membrane filter (Sartorious, AG Germany) after 1, 3, 5, 10, 15, 30, 45, 60, 90 min and replaced with an equivalent amount of the fresh dissolution medium. Concentrations of mosapride citrate were determined by reverse phase HPLC. All experiments were done in triplicate.

Dissolution profiles were evaluated by calculating the dissolution efficiency parameter at 60 min (DE_{60min}), from the area under the dissolution curve, according to the method of Khan.[20] Additionally, the initial dissolution rate (IDR, % dissolved/min) was computed over the first 5 min of dissolution.

Two-way analysis of variance (ANOVA) was performed to determine the significance of difference between the DE_{60min} data of the binary systems to test the significance of the effects of the preparation method and CD type. The level of significance was set at p value of ≤0.05 using SPSS version 12.0 software computer program.

Results and discussion

Phase solubility study

The phase solubility profiles for the drug-CDs inclusion complexes are presented in Figure 2.

They displayed A_L type[18] equilibrium phase solubility diagrams for both mosapride citrate-β-CD and mosapride citrate-$SBE_7\beta$-CD binary systems, showing that mosapride citrate solubility increases linearly as a function of CD concentrations and that soluble complexes were formed without occurrence of precipitation in the range of CD concentrations used. The linear host guest correlation with slope of less than 1 suggested the formation of a 1:1 complex with respect to both β-CD and $SBE_7\beta$-CD concentrations.

The values of CE and $K_{1:1}$ of mosapride citrate-β-CD and mosapride citrate-$SBE_7\beta$-CD inclusion complexes are presented in Table 1.

The CE of $SBE_7\beta$-CD (1.486) was higher than that of β-CD (0.069) because the charged groups of $SBE_7\beta$-CD

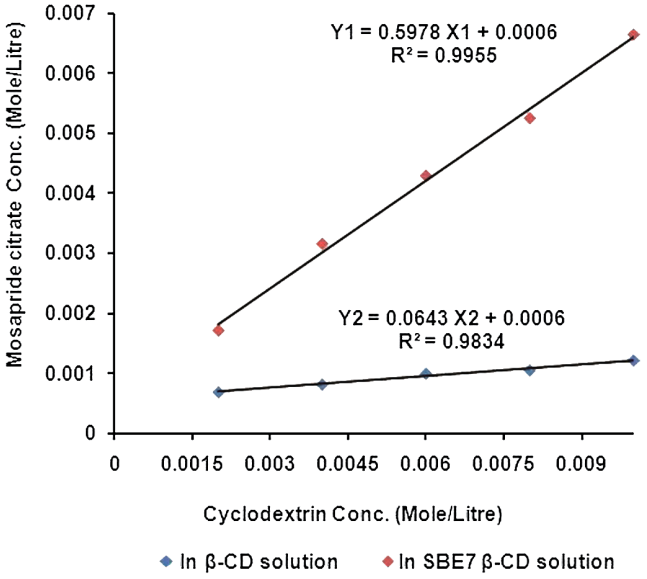

Figure 2. Phase solubility profiles for the inclusion complexes mosapride citrate-β-CD and mosapride citrate-$SBE_7\beta$-CD. (See colour version of this figure online at www.informahealthcare.com/phd)

Table 1. Values of CE and $K_{1:1}$ of inclusion complexes of mosapride citrate-β-CD and mosapride citrate-$SBE_7\beta$-CD.

β-CD conc. (mole/L)	Mosapride citrate conc. (mole/L) (Average ± S.D)	$SBE_7\beta$-CD conc. (mole/L)	Mosapride citrate conc. (mole/L) (Average ± S.D)
0.002	0.00069 ± 8.39E-07	0.002	0.00171 ± 2.36E-05
0.004	0.00082 ± 4.25E-07	0.004	0.00315 ± 4.82E-05
0.006	0.00099 ± 2.89E-07	0.006	0.00429 ± 2.71E-05
0.008	0.00105 ± 5.62E-07	0.008	0.00525 ± 2.14E-05
0.01	0.00122 ± 1.61E-07	0.01	0.00664 ± 3.78E-05
Slope = 0.0643		Slope = 0.5978	
Intercept = 0.0006		Intercept = 0.0006	
[a]CE = 0.069		[a]CE = 1.486	
R^2 = 0.9955		R^2 = 0.9834	
[b]$K_{1:1}$ = 114.53 $mole^{-1}$		[b]$K_{1:1}$ = 2477.21 $mole^{-1}$	

[a]CE: Complexation efficiency.
[b]$K_{1:1}$: Stability constant.
R^2: Correlation coefficient
S.D: Standard deviation.

are appropriately spaced from the cavity and the hydrophobicity around the cavity increases due to the presence of alkyl chains[21].

Therefore, $K_{1:1}$ values of $SBE_7\beta$-CD inclusion complex (2477.21 $mole^{-1}$) was greater than that obtained with β-CD (114.53 $mole^{-1}$) since the complexation with the $SBE_7\beta$-CD involves the CD cavity, as well as the hydrophobic butyl side arms that extend the hydrophobic cavity of the CD.

Superior CD complexation efficiency may prove advantageous during dosage form design, and would therefore appear to be a potential advantage for $SBE_7\beta$-CD.

Preparation of drug-CDs inclusion complexes

Solid binary systems of mosapride citrate with β-CD and $SBE_7\beta$-CD were prepared using physical mixing, kneading and freeze drying techniques. The conventional 1:1 molar ratio[22–24] was chosen for the preparation of solid binary systems.

Physicochemical characterization of the prepared inclusion complexes

X-ray diffractometry

The XRD patterns for pure drug and its binary systems prepared by different techniques at molar ratio of 1:1 are represented in Figures 3 and 4, respectively.

The diffraction pattern of mosapride citrate powder revealed several sharp high-intensity peaks at diffraction angles of 8.47°, 4.88°. 4.24°, 3.89°, 3.75°, 3.72° and 2.95° suggesting that the drug existed as crystalline material.

X-ray diffraction patterns of mosapride citrate with both β-CD and $SBE_7\beta$-CD physical mixtures were practically constituted by the superposition of the spectra of the single components, indicating no formation of new structure. However, lower intensities of the diffraction peaks were observed due to particle size reduction during mixing and dilution of the pure crystalline components[25].

The diffraction pattern of mosapride citrate with β-CD kneaded system presented a quite similar to that of freeze

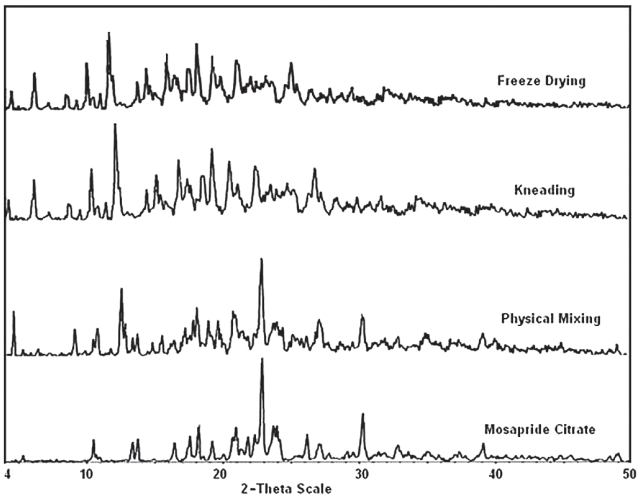

Figure 3. X-ray diffraction patterns of mosapride citrate-β-CD binary mixtures prepared by different methods.

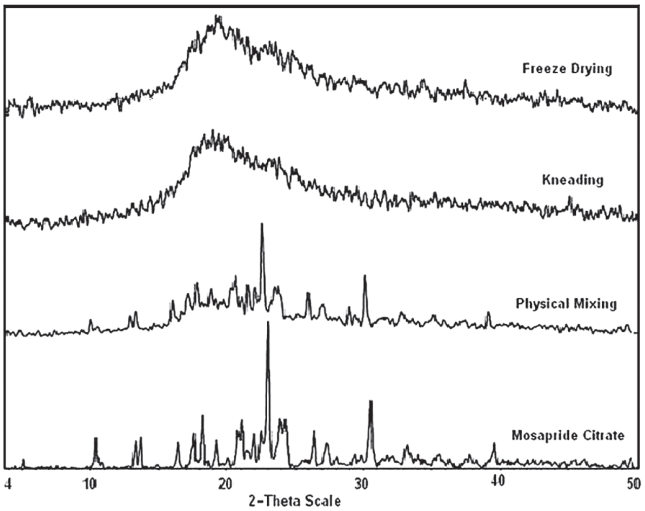

Figure 4. X-ray diffraction patterns of mosapride citrate-$SBE_7\beta$-CD binary mixtures prepared by different methods.

drying showed few, broad and less intense peaks revealed drug amorphousness.

The presence of the drug peaks in the diffractogram obtained from β-CD freeze dried system could suggest the presence of the free crystalline drug, although reduction in number and intensities were observed.

On the other hand, the diffractograms of both kneaded and freeze dried systems prepared using SBE$_7\beta$-CD showed a typical diffuse pattern indicating the entirely amorphous nature of mosapride citrate in both systems.

According to Williams et al.[26] lack of crystallinity is an added evidence for the formation of inclusion complex. However, since the amorphousness of the drug can be a sequence of the lyophilization process, it is possible that the X-ray data cannot discriminate whether the drug-CDs lyophilized systems obtained are true inclusion complexes or homogenous dispersed mixtures of the amorphous components.[27]

Differential scanning calorimetry

Thermal analysis may give some evidence of inclusion complexation. When the guest molecules are embedded in CD cavities or in the crystal lattice, their melting, boiling or sublimation points generally shift to a different temperature or disappear within the temperature range where CD is decomposed.[28]

The DSC thermograms of pure components and different binary systems are presented in Figures 5 and 6. The mosapride citrate thermogram was typical of a crystalline substance with a fusion endothermic peak at 214.11°C, corresponding to the melting point of the drug.

The drug endothermic peak in the DSC thermograms of physical mixing systems; is clearly distinguishable indicating that in such systems the drug has basically maintained its original crystallinity.[29]

In the DSC thermograms of the freeze dried systems prepared using β-CD and SBE$_7\beta$-CD the drug endothermic melting peak completely disappeared. This could indicate amorphous solid dispersion or molecular encapsulation of the drug into the CD cavity.[30]

Fourier-transform infrared (FTIR) spectroscopy

More evidence of complex formation was obtained from FTIR study, which investigated the functional groups of mosapride citrate involved in the complexation.

The FTIR spectra of pure components and their binary systems prepared by different techniques at molar ratio of 1:1 (drug to CD) are shown in Figures 7 and 8.

The FTIR spectrum of mosapride citrate showed one characteristic forked absorption band at 3443.28 and 3379.64 cm^{-1} corresponding to –NH$_2$ stretching vibration and another one characteristic forked absorption band at 3334.32, 3226.33 cm^{-1} corresponding to tertiary amine (–CO*NH*) stretching vibration.

There is also a characteristic absorption band at 1723.09 cm^{-1} corresponding to the carbonyl amido (–*CO*NH) stretching vibration. Other sharp bands appeared at 1249.65 cm^{-1} (C–Cl stretching), 1214.23 cm^{-1} (C–F stretching), 1628.59 (C–N stretching) and 1546.63 cm^{-1} (C–H stretching).

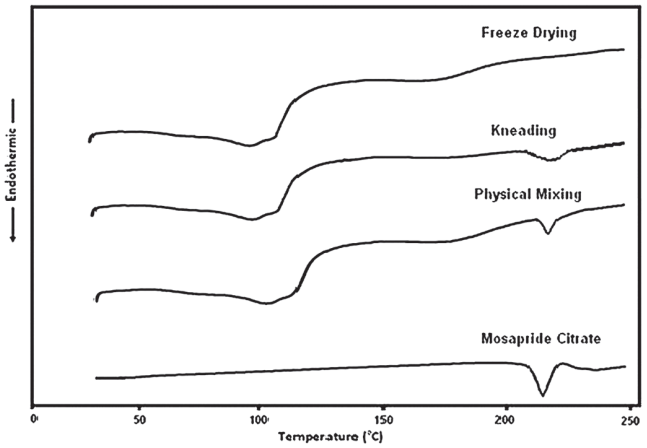

Figure 5. DSC thermograms of mosapride citrate-β-CD binary mixtures prepared by different methods.

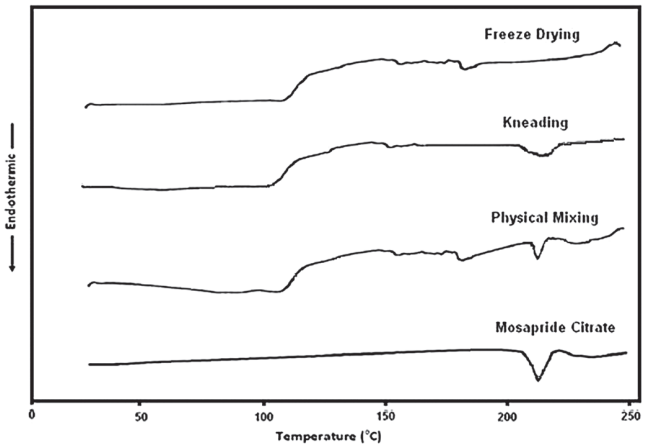

Figure 6. DSC thermograms of mosapride citrate-SBE$_7\beta$-CD binary mixtures prepared by different methods.

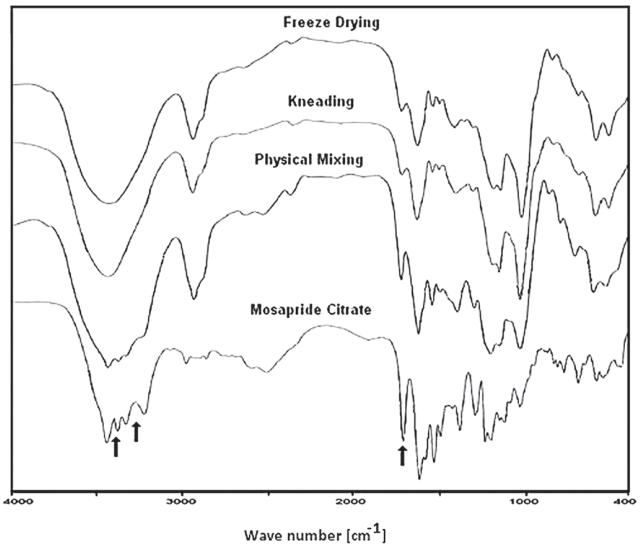

Figure 7. IR patterns of mosapride citrate-β-CD binary mixtures prepared by different methods.

In this study the characteristic (–NH$_2$) and (–CO*NH*) stretching band of mosapride citrate were masked in

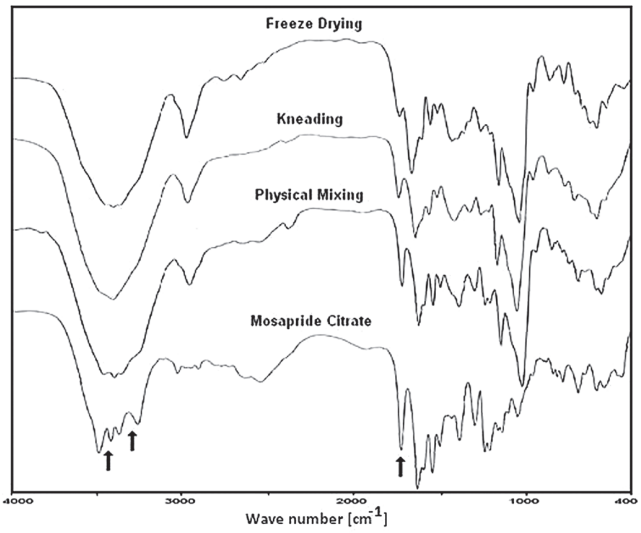

Figure 8. IR patterns of mosapride citrate-SBE$_7\beta$-CD binary mixtures prepared by different methods.

all the prepared systems by the broad intense band corresponding to the free–OH vibration of CD (3500–3200 cm^{-1}). Also, there was an overlap between the carbonyl stretching of the drug at 1723.09 cm^{-1} and the band corresponding to the hydrated bonds within CD molecules at (1750–1650 cm^{-1}).

Therefore, the characteristic stretching bands of (–CO*NH*) and the carbonyl stretching (–*CO*NH) of mosapride citrate at 1723.09 cm^{-1} were the main characteristic bands used to assess the drug-CD interactions.

The FTIR spectra of all the physical mixing and the kneading products did not show any significant changes with respect to the FTIR spectra of the pure components, and in particular the characteristic carbonyl stretching band of mosapride citrate.

On the other hand, the FTIR spectra of the freeze drying products exhibited a broadening and decrease in intensity of the characteristic mosapride citrate carbonyl stretching band. A significant decrease in intensity occurred in the binary mixtures with SBE$_7\beta$-CD prepared by freeze drying technique. The broadening and decrease in the intensity of the drug carbonyl stretching band observable in these systems might be due to its restriction within the CD cavity.[31]

Scanning electron microscopy

SEM microphotographs of pure mosapride citrate, pure SBE$_7\beta$-CD and mixtures prepared by physical mixing, kneading and freeze drying method using SBE$_7\beta$-CD are presented in Figure 9.

Microphotograph (A) of pure drug showed a drug in different polymorphic crystalline structures (spherical and elongate crystals), while microphotograph (B) showed the spherical particles of SBE$_7\beta$-CD with numerous cavities.

Concerning the drug-SBE$_7\beta$-CD mixtures prepared by different techniques, in microphotograph (C) we can distinguish between the drug and polymer particles where the drug is deposited in the cavities and between the polymer particles in the crystalline state, while solid dispersion prepared by kneading (microphotograph D) there are some small fine recrystallized particles attributed to mosapride citrate are present in the pores of larger crystalline mass.

On the other hand, the sample prepared by freeze drying (microphotograph E) presented a clearly different appearance since both drug and polymer was recrystallized together with high reduction in the visible drug observed in the solid dispersion.

This could be attributed to the inclusion of the drug in the polymer matrix as confirmed in the XRD studies.

Determination of solubility of mosapride citrate-CDs inclusion complexes

For pure mosapride citrate, the drug solubility was found to be 0.095 mg/mL. The solubility results of mosapride citrate-CDs inclusion complexes demonstrated that the mean amount of drug dissolved in phosphate buffer solution (pH 6.8) was found to be 0.546, 1.035 and 1.433 mg/mL for β-CD inclusion complexes prepared by physical mixing, kneading and freeze drying method respectively (Table 2).

Concerning SBE$_7\beta$-CD inclusion complexes prepared by physical mixing, kneading and freeze drying method the drug solubility was higher and found to be 1.407, 5.906 and 7.859 mg/mL, respectively (Figure 10).

There is a marked increase in the solubility of inclusion complexes prepared by different methods using both β-CD and SBE$_7\beta$-CD compared to pure drug. Also, there is a marked increase in the solubility of inclusion complexes prepared with kneading and freeze drying methods compared to those prepared with physical mixing method. This effect is attributed to inclusion into the cavity of CDs with reduction in the crystallinity of the drug caused by kneading and freeze-drying methods.

In vitro dissolution studies

Mosapride citrate dissolution profiles from its pure powder and binary systems with CDs in simulated saliva solution (pH 6.8) are demonstrated in Figures 11 and 12. The percent dissolved was calculated according to predetermined drug content for each product.

The dissolution efficiency data calculated based on 60 min ($DE_{60\ min}$) and the initial dissolution rate during the first 5 min (IDR) of all the systems are compiled in Table 3.

The dissolution profile of mosapride citrate from its pure powder showed $DE_{60\ min}$ value of 53.48 % and IDR of 5.47 % indicating that incomplete dissolution which could be due to less wettability of the powder.

It was evident that the mosapride citrate dissolution was enhanced when physically mixed with CDs due to local solubilization action of the carrier operating in the microenvironment of the drug, or the hydrodynamic

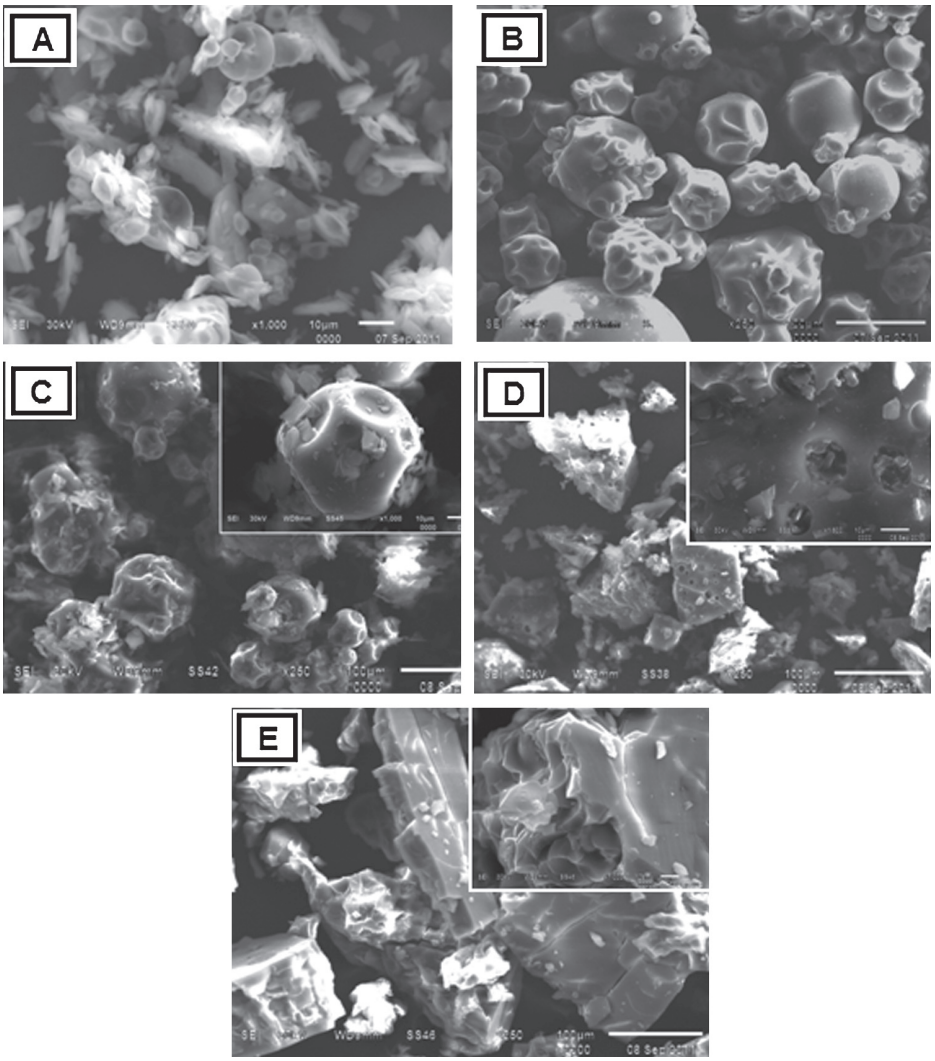

Figure 9. SEM microphotographs of (a) pure mosapride citrate, (b) pure SBE$_7$$\beta$-CD, (c) mosapride citrate-SBE$_7$$\beta$-CD mixture (prepared by physical mixing), (d) mosapride citrate-SBE$_7$$\beta$-CD mixture (prepared by kneading method) and (d) mosapride citrate-SBE$_7$$\beta$-CD mixture (prepared by freeze-drying method.

layer surrounding drug particles in the early stages of the dissolution process, since CDs dissolve in a short time. This action resulted in an *in-situ* inclusion process causing a rapid increase in the amount of dissolved.

The $DE_{60\ min}$ values of β-CD and SBE$_7$$\beta$-CD inclusion complexes prepared by physical mixing were 64.46 and 72.24 % respectively. The increase in the drug dissolution rate from physical mixtures could be, to a lesser extent, due to the surfactant like properties of CDs, which reduce the interfacial tension between the water insoluble drug particles and the dissolution medium, thus improving the wettability and dissolution of the drug.[32]

It was obvious that the freeze dried systems showed marked increase in mosapride citrate dissolution compared with the other methods, showing a burst effect of more than 80 % during the first 5 min that could be attributed mainly to the formation of soluble inclusion complexes of the drug with CDs and the high energetic amorphous state or reduction of the crystallinity following complexation as reported previously.[33]

Table 2. Solubility values of pure mosapride citrate and its CDs inclusion complexes prepared by different methods.

CD type	Method	Solubility (mg/mL) ± S.D
β-CD	Physical mixing	0.546 ± 0.07
	Kneading	1.035 ± 0.16
	Freeze drying	1.443 ± 0.21
SBE$_7$$\beta$-CD	Physical mixing	1.407 ± 0.08
	Kneading	5.906 ± 0.19
	Freeze drying	7.859 ± 0.10
Mosapride citrate		0.095 ± 0.14

Additionally, Betageri and Makarla[34] stated that the marked increase in the dissolution rate might be due to the formation of solid solution of the drug in the freeze dried products as a result of the complete inclusion of the drug into the CD cavities. The particle size was reduced to the molecular size when the carrier brought the drug into the dissolution medium, leading to fast dissolution.

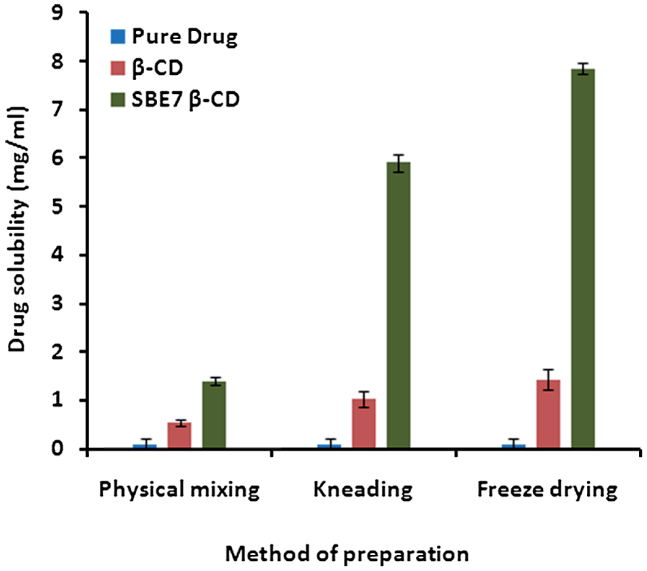

Figure 10. Solubilities of pure mosapride citrate and its binary mixtures prepared by different methods using β-CD and SBE$_7\beta$-CD. (See colour version of this figure online at www.informahealthcare.com/phd)

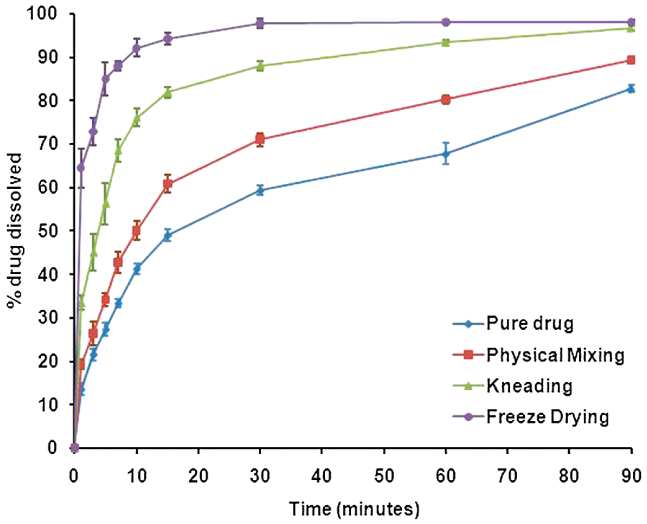

Figure 11. Dissolution profiles of mosapride citrate binary mixtures prepared by different methods using β-CD. (See colour version of this figure online at www.informahealthcare.com/phd)

In addition to the preparation method, the effect of the CD type was also evident on the dissolution of mosapride citrate, where the solid binary systems prepared using SBE$_7\beta$-CD exhibited superior enhancement in drug dissolution compared with that prepared using the parent β-CD, especially on using the freeze dried technique (IDR of 19.43%).

This could be explained on the basis of greater water solubility, better wetting ability and higher complexing power of β-CD derivative towards the drug in the solid state.

The previous findings are in perfect agreement with the values of CE obtained for mosapride citrate with the used CDs.

The results of the two-way ANOVA performed on the DE $_{60min}$ data revealed the presence of significant

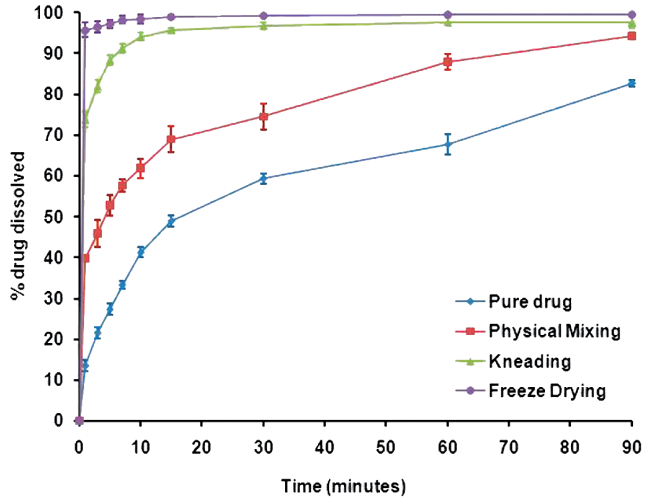

Figure 12. Dissolution profiles of mosapride citrate binary mixtures prepared by different methods using SBE$_7\beta$-CD. (See colour version of this figure online at www.informahealthcare.com/phd)

Table 3. Values of IDR and DE $_{60\,min}$ of the release profiles of binary mixtures with CDs prepared by different methods.

CD type	Method	IDR (% dissolved/min) ± S.D	DE $_{60\,min}$ (%) ± S.D
β-CD	Freeze drying	16.99 ± 0.74	93.59 ± 0.90
	Kneading	11.27 ± 0.94	82.13 ± 0.66
	Physical mixing	6.83 ± 0.28	64.46 ± 1.08
SBE$_7\beta$-CD	Freeze drying	19.43 ± 0.20	98.10 ± 0.54
	Kneading	17.76 ± 0.23	94.22 ± 0.53
	Physical mixing	10.56 ± 0.50	72.24 ± 1.93
Pure drug		5.47 ± 0.28	53.48 ± 0.84

[a]IDR: Initial dissolution rate.
[b]DE $_{60\,min}$: Dissolution efficiency.

differences among the different preparation methods at the same CD at $p \le 0.05$ (p_{value} = 2.84E-06 and 3.71E-05 for β-CD methods and SBE$_7\beta$-CD methods, respectively).

Also there is a significant differences between β-CD and SBE$_7\beta$-CD in physical mixing, kneading and freeze-drying methods at $p \le 0.05$ (p_{value} = 0.013, 0.002 and 0.005 for physical mixing, kneading and freeze-drying methods, respectively).

Conclusion

Solid binary systems of mosapride citrate with β-CD and SBE$_7\beta$-CD were prepared using physical mixing, kneading and freeze-drying techniques in 1:1 (drug:CD) molar ratios. From the above results, it is possible to conclude that both β-CD and SBE$_7\beta$-CD were able to form true inclusion complexes with mosapride citrate at a molar ratio of 1:1 using the freeze-drying technique. The dissolution of mosapride citrate was markedly enhanced in both systems, showing an initial burst effect of more than 80 % in the first 5 min. A significant difference was found between the two systems at $p \le 0.05$. Therefore, the freeze dried system of mosapride citrate with SBE$_7\beta$-CD prepared at a molar ratio of 1:1

could be chosen for the formulation of mosapride citrate mucoadhesive buccal tablets.

Acknowledgments

The authors wish to acknowledge Marcyrl pharma (Egypt) for the provision of Mosapride citrate. The authors are grateful to Cydex pharmaceuticals (USA) for providing SBE$_7$$\beta$-CD as a gift sample. The authors are also grateful to Roquette (France) for the gift sample of β-CD.

Declaration of interest

The authors report no declarations of interest.

References

1. Junko E, Masahiro N, Satofumi M, Nobutaka U. Influence of mosapride citrate on gastric motility and autonomic nervous function: Evaluation by spectral analyses of heart rate and blood pressure variabilities, and by electrogastrography. J Gastroenterol 2002;37:888–895.
2. Liu Z, Sakakibara R., Odaka T. Mosapride citrate, a novel 5-HT4 agonist and partial 5-HT3 antagonist, ameliorates constipation in parkinsonian patients. Mov Disord 2005;20:680–686.
3. Futagami S, Iwakiri K, Shindo T, Kawagoe T, Horie A, Shimpuku M. The prokinetic effect of mosapride citrate combined with omeprazole therapy improves clinical symptoms and gastric emptying in PPI-resistant NERD patients with delayed gastric emptying. J Gastroenterol 2010;45:413–421.
4. Kim H, Choi E. The effect of mosapride citrate on proximal and distal colonic motor function in the guinea pig in vitro. Neurogastroenterol Motil 2008;20:169–176.
5. Sun X, Niu L, Li X, Lu X, Li F. Characterization of metabolic profile of mosapride citrate in rat and identification of two new metabolites: Mosapride *N*-oxide and morpholine ring opened mosapride by UPLC–ESI-MS/MS. J Pharm Biomed Anal 2009;50:27–34.
6. Kato S, Morie T, Kon T, Yoshida N, Karasawa T, Matsumoto J. Novel benzamides as selective and potent gastrokinetic agents. 2. Synthesis and structure-activity relationships of 4-amino-5-chloro-2-ethoxy-N- [[4-(4-fluorobenzyl)-2-morpholinyl] methyl] benzamide citrate (AS-4370) and related compounds. J Med Chem 1991;34:616–624.
7. Loftsson T, Byskov S, Brewster ME, Konrádsdóttir F. Effects of cyclodextrins on drug delivery through biological membranes. J Pharm Sci 2007;96:2532–2546.
8. Derle D, Boddu SHS, Mager M. Studies on the preparation, characterization and solubility of β-cyclodextrin-starnidazole 7 inclusion complexes. Indian J Pharma Edu Res 2006;40:232–236.
9. Govindrajan R, Nagarsenker MS. Influence of preparation methodology on solid state properties of an acidic drug-cyclodextrin system. J Pharmcol 2004;56:725–733.
10. Govindrajan R, Nagarsenker MS. Formulation studies and in vivo evaluation of a flurbiprofen-hydroxypropyl β-cyclodextrin system. Pharmaceut Dev Tech 2005;1:105–114.
11. Baboota S, Dhariwal M, Kohli K. Physicochemical characterization, *in vitro* dissolution behavior and phamacodynamic studies of refecoxib cyclodextrin inclusion compound. Preparation and properties of refecoxib hydroxypropyl β-cyclodextrin inclusion complex. AAPS Pharma Sci Tech 2005;6:83–90.
12. Baboota S, Agrawal SP. Inclusion complexation of meloxicam with β-cyclodextrin. Indian J Pharma Sci 2002;64:408–411.
13. Longxiao L, Suyan Z. Preparation and characterization of inclusion complexes of prazosin hydrochloride with β-cyclodextrin and hydroxypropyl β-cyclodextrin. J Pharm Biomedical Anal 2006;40:122–127.
14. Ning L, Yun-Hui ZYN Wu, Xiao-Li X, Ya-Hui Z. Inclusion complex of trimethoprin with β-cyclodextrin. J Pharm Biomedical Anal 2005;39:824–829.
15. Singh R, Bharti N, Madan J, Hiremath SN. Characterization of cyclodextrin inclusion complexes: A review. J Pharm Sci Tech 2010;2:171–183.
16. Rao VM, Haslam JL, Stella VJ. Controlled and complete release of a model poorly water-soluble drug, prednisolone, from hydroxyl propyl methyl cellulose matrix tablets using SBE-β-cyclodextrin as a solubilizing agent. J Pharm Sci 2001;90:807–816.
17. Mosher G, Thompson DO. (2002). Complexation and cyclodextrins. In: Swarbrick J, Boylan JC, eds. Encyclopedia of Pharmaceutical Technology. New York: Marcel Dekker, 531–558.
18. Higuchi T, Connors KA. (1965). Phase solubility techniques. In: Reilly CN, ed. Advances in Analytical and Chemistry Instrumentation, Vol. 4. New York: Wiley Interscience, 117–212.
19. Loftsson T, Matthíasson K, Másson M. The effects of organic salts on the cyclodextrin solubilization of drugs. Int J Pharm 2003;262:101–107.
20. Khan KA. The concept of dissolution efficiency. J Pharm Pharmacol 1975;27:48–49.
21. Loftsson T, Duchêne D. Cyclodextrins and their pharmaceutical applications. Int J Pharm 2007;329:1–11.
22. Jain NK. Progress in controlled and novel drug delivery system. Cyclodextrin Based Drug Del Sys, 2004;1:384–400.
23. Erden N, Celebi N. A study of the inclusion complex of naproxen with β-cyclodextrin. Int J Pharma 1988;48:83–89.
24. Derle D, Boddu SHS, Magar M. Studies on the preparation, characterization and solubility of betacyclodextrin satranidazole inclusion complexes. Indian J Pharm Educ Res 2006;40:232–236.
25. Ribeiro LSS, Ferreira DC, Veiga FJB. Physicochemical investigation of the effects of water-soluble polymers on vinpocetine complexation with β-cyclodextrin and its sulfobutyl ether derivative in solution and solid state. Eur J Pharm Sci 2003;20:253–266.
26. Williams RO, Mahaguna V, Sriwongjanya M. Characterization of an inclusion complex of cholesterol and hydroxypropyl-β-cyclodextrin. Eur J Pharm Biopharm 1998;46:355–360.
27. Sauceau M, Rodier E, Fages J. Preparation of inclusion complex of piroxicam with cyclodextrin by using supercritical carbon dioxide. J Supercrit Fluids 2008;47:326–332.
28. Cabral Marques H, Hadgraft J, Kllaway I. Studies of cyclodextrin inclusion complexes. I. The Salbutamol cyclodextrin complex as studied by phase solubility and DSC. Int J Pharm 1990;63:259–266.
29. Ning L, Zhang YH, Wu Ya-Nan, Xiong XL, Zhang YH. Inclusion complex of trimethoprim with β-cyclodextrin. J Pharm Biomed Anal 2005;39:824–829.
30. Mura P, Adragna E, Rabasco AM, Moyano JR, Pérez-Martìnez JI, Arias MJ et al. Effects of the host cavity size and the preparation method on the physicochemical properties of ibuproxam-cyclodextrin systems. Drug Dev Ind Pharm 1999;25:279–287.
31. Ficarra R, Ficarra P, Di Bella MR, Raneri D, Tommasini S, Calabrò, ML et al. Study on the inclusion complex of atenolol with β-cyclodextrin. J Pharm Biomed Anal 2000;23:231–236.
32. Moyano JR, Gines JM, Arias MJ, Rabasco AM. Study of the dissolution characteristics of oxazepam via complexation with β-cyclodextrin. Int J Pharm 1995;114:95–102.
33. Dollo G, Corre P, Chollet M, Chevanne F, Bertault M, Burgot JL et al. Improvement in solubility and dissolution rate of 1,2-dithiole-3-thiones upon complexation with β-cyclodextrin and its hydroxypropyl and sulfobutyl ether-7 derivatives. J Pharm Sci 1999;88:889–895.
34. Betageri GV, Makarla KR. Enhancement of dissolution of glyburide by solid dispersion and lyophilization techniques. Int J Pharm 1995;126:155–160.